Ecological significance of the environmental heterogeneity between the upper and lower surfaces of a single leaf as a determinant of acarine predator–prey relationship

SUDO Masaaki

Graduate school of Agriculture
KYOTO UNIVERSITY

2014

Table of contents

Chapter 1
General introduction

Plants have evolved diverse topographies between adaxial (upper) and abaxial (lower) leaf surfaces, e.g., in possession of leaf domatia (O'Dowd and Willson 1989; Nishida 2004), hair density and shape (Chien and Sussex 1996), wax and cuticle layer thickness (Price 1980), and stomatal density (Gutschick 1999). Such structures influence microclimates and cause differences in temperature and humidity (Grostal and O'Dowd 1994; Gutschick 1999; cf. Weintraub et al. 2007). As a result, adaxial and abaxial leaf surfaces offer heterogeneous environments for plant-dwelling arthropods, affecting behavior of inhabitants and their (inter-specific) interactions, e.g., foraging efficiency in predatory mites (Krips et al. 1999).

The two surfaces of a plant leaf also correspond to the upper and the lower sides unless it projects vertically. Consequently, mites on leaves will experience upward or downward gravitational pull, which affects within-plant distribution (Li and Margolies 1991) and fecundity (Sakai et al. 2012a) of spider mites. Additionally, leaves function as protective shields against solar ultraviolet (UV) radiation by accumulating phenolic compounds such as flavonoids (Izaguirre et al. 2007). The heterogeneity in UV radiation leads to differences in abundance of phylloplane fungi between upper and lower leaf surfaces (Newsham et al. 1997).

Fine structures on leaf surfaces can play important roles in structuring arboreal mite assemblages. In general, shelter availability (domatia and dense trichomes) for mites, especially for predatory phytoseiid mites, is higher on the abaxial than the adaxial leaf surfaces (O'Dowd and Willson 1989; Kreiter et al. 2003; Sudo et al. 2010). Domatia protect mites from low humidity and from inter- and/or intraguild predators (Grostal and O'Dowd 1994; Norton et al. 2001; Kasai et al. 2005). In addition, pubescences on leaves trap pollen and/or fungal spores, alternative food resources of generalist phytoseiid mites, and contribute their population viability on trees (McMurtry and Croft 1997; Kreiter et al. 2002; Roda et al. 2003; but see Duso et al. 2004). The population densities of phytoseiids and some fungivorous mites, such as Winterschmidtiidae or Tydeoidea, were positively correlated with density of hairs and leaf domatia (Karban et al. 1995; O'Dowd and Willson 1997; O'Dowd and Pemberton 1998; Sudo et al. 2010).

Living on an upper leaf surface have been considered to be harsh to mites in comparison with on a lower leaf surface because of rainfall or submergence, which decreases survivability of spider mites (both eggs and motile individuals) (Tanaka and Inoue 1962; Foott 1963; Osakabe 1967; Ikegami et al. 2000). Recent studies have asserted that intra-leaf distribution in spider mites and phytoseiid mites is biased to the lower leaf surfaces to avoid solar ultraviolet-B (UVB, 280–320 nm wavelengths) radiation (Ohtsuka and Osakabe 2009; Suzuki et al. 2009; Onzo et al. 2010), which

is harmful for both mite eggs and motile individuals (Barcelo 1981; Sakai and Osakabe 2010). Nevertheless, potential impacts of the heterogeneous habitats between adaxial and abaxial (upper and lower) surfaces on the spatiotemporal structure and intra- and interspecific interactions have hardly been addressed on a foliar acarine community.

The habitat heterogeneity between upper and lower leaf surfaces may distinctively exert the effects on the leaf-surface utilization patterns of phytoseiid mites and spider mites. As shelter (hairs and domatia) availability and food abundance promote the priority of the lower (abaxial) leaf surfaces as habitats for phytoseiids to the upper surfaces, spider mites possibly reduce predation risk if they can remain on the upper leaf surface. In this study, I investigated whether the environmental heterogeneity relevant to upper and lower leaf surfaces segregated the spatial distribution of acarine predator and prey within a single leaf and how the environmental and biological factors function in their interspecific interaction.

Prior to the present study, I surveyed the seasonal dynamics of foliar mite assembly on a deciduous shrub, *Viburnum erosum* Thunb. var. *punctatum* Franch. et Sav. (Adoxaceae; VEP), and other 14 sympatric tree/shrub species of secondary forest on the outskirts of Kyoto (Sudo et al. 2010). Leaves of VEP have stellate hairs on both of adaxial and abaxial surfaces and leaf domatia (hair tufts) on vein axils of abaxial surface. The VEP leaves maintain populations of fungivorous mites (Winterschmidtiidae and Tydeoidea) and predatory mites (phytoseiids) from May to November in each year (Sudo et al. 2010). Therefore, VEP leaves are considered to be suitable substrata to investigate the leaf-surface utilization patterns relevant to various mite taxa and their seasonal fluctuations. On the other hand, the occurrence of herbivorous mites on VEP leaves was seasonally limited; a false spider mite, *Brevipalpus obovatus* Donnadieu (Acari: Tenuipalpidae), was observed only in autumn (September to October).

In Chapter 2, the two-year dataset obtained by the abovementioned field survey of Sudo et al. (2010) was re-analyzed. The leaf-surface distribution patterns of mites were compared among their trophic groups (mite taxa), surface architecture (presence/absence of domatia and hairs) of host plant leaves, or leaves collected from the same plant in different seasons. While the majority of mite taxa on VEP and sympatric plants, including Phytoseiidae, commonly showed an abaxial-biased distribution, *B. obovatus* distributed and oviposited both on the adaxial and abaxial leaf surfaces of VEP leaves.

In the following three chapters (3–5), the oviposition on upper leaf surface of VEP by *B. obovatus* was examined from the aspects of anti-predator and anti-stress adaptations. Chapter 3 clarified how the difference in surface morphology (forms of stellate hairs) between the adaxial and the abaxial surfaces of VEP leaves affected the predator–prey interaction in foliar mite community. The stellate hair structure is more developed (having more ramifications) on the abaxial surface than adaxial surfaces; fecundity and egg survival of *B. obovatus* were significantly improved on the abaxial leaf

surface in the presence of a generalist predator, *Phytoseius nipponicus* Ehara (Acari: Phytoseiidae), in comparison with the adaxial surface.

Chapter 4 addressed the effects of leaf-surface preferences of the two mite species on the predator–prey interaction on VEP leaves. *Phytoseius nipponicus* showed positive geotaxis and a preference for the abaxial surface over the adaxial surface of VEP leaves, whereas *B. obovatus* had negative geotaxis and a preference for surface environments on the adaxial leaf surfaces. The resulting spatial segregation reduced opportunities for encounters between the predator and the prey, thereby the indirect negative effect of predator presence on prey fecundity and the risk of egg predation were alleviated.

Chapter 5 quantified the lethal effects of environmental stresses on the egg survival of *B. obovatus* on the upper leaf surface. Both of the temperature condition (solar radiant heat) and solar UVB irradiance during the egg period in each season restricted the availability of upper leaf surfaces as oviposition site; they were considered to contribute the limited seasonal occurrence of *B. obovatus* on VEP leaves in autumn.

Finally, I synthetically discussed whether the heterogeneous environments on the upper (adaxial) and the lower (abaxial) surfaces of a VEP leaf segregated the spatial distribution of *P. nipponicus* and *B. obovatus*, how the environmental and biological factors function in the predator–prey interaction, and contribution of the heterogeneous environments toward population survival of the prey on a predator-rich host plant leaf in Chapter 6 (general discussion).

Chapter 2
Intra-leaf distribution of plant mites in temperate broadleaf forest

2-1 Introduction

Divergent strategies to overcome the direct and indirect effects of environmental stress are potentially relevant to adaxial/abaxial leaf surface exploitation and distribution patterns of arthropod communities. However, the between-surface distributions were scarcely taken into consideration even in literatures that addressed the effects of structure and/or architecture of foliage on abundance and behavior of arthropods (Johnson 1975; Walter 1996). Few datasets are available to analyze the exploitation and distribution patterns of arthropods between the leaf surfaces.

In a temperate forest in Kyoto, woody plant species bearing domatia and/or trichomes such as VEP harbored more mites than those without such microstructures (Sudo et al. 2010). Major mite taxa found on VEP were the predacious family Phytoseiidae, the herbivorous superfamily Eriophyoidea, the fungivorous family Winterschmidtiidae, and the fungivorous (Walter and Proctor 1999) superfamily Tydeoidea (Sudo et al. 2010). In this chapter, I inspected the effects of leaf morphology and seasons on the adaxial–abaxial leaf-surface distribution of mites on VEP and other sympatric tree and shrub species using the dataset of the field investigation by Sudo et al. (2010). Additionally, I investigated diel changes in the intra-leaf distribution of mites on VEP in the field.

2-2 Materials and methods

2-2-1 Dataset for intra-leaf distribution analysis

Study site and plants

The dataset, originally taken for Sudo et al. (2010), was re-analyzed to compare intra-leaf mite distribution between plants with different leaf-surface morphologies (section 2-2-2) and to investigate the seasonal changes in intra-leaf distribution of various mite taxa on VEP (section 2-2-3). Sudo et al. (2010) sampled mites from two sites in secondary broadleaf forests on the outskirts of Kyoto, Japan: Uryu-yama (35°2'8"N, 135°47'53"E, 110–150 m a.s.l.) and Iwakura (35°5'28"N, 135°46'42"E, 150–160 m a.s.l.) for two years, 2007–2008. The study site in the Uryu-yama was located along a 50-m-long trail on a spur; *Eurya japonica* Thunb. (Theaceae), *Rhododendron macrosepalum*

Maxim. (Ericaceae), and VEP dominated the understory in a forest whose canopy was dominated by *Quercus serrata* Thunb. and *Q. glauca* Thunb. (Fagaceae). The study site in Iwakura was located alongside a 100-m-long unshaded road; VEP and *Sasa* sp. (Poaceae) dominated the understory in a forest whose canopy was dominated by *Pinus densiflora* Siebold et Zucc. (Pinaceae) and *Q. serrata*.

In March 2007, eleven VEP shrubs were randomly selected in each study site. However, because six VEP shrubs were felled in the course of the 2-year survey, six neighboring VEP shrubs were newly selected for subsequent samplings. In early August 2007, 29 trees or shrubs of 14 woody species were selected from the vicinity of the target VEP shrubs; nine of the selected plants were lost due to felling or blight by June 2008. Consequently, 20 individuals were added to normalize the number of replication among the categories of leaf surface morphology, and 148 individual plants in total other than VEP were used (Table 2-1).

Mite sampling method for "comparison of intra-leaf mite distribution among 15 woody plant species" (2-2-2)

Mites sampled from the Uryu-yama site were used for the comparison of intra-leaf distribution between plant species with different leaf morphology. Mite sampling in Uryu-yama from plant species except for VEP was conducted four times (August 2007, June 2008, August 2008, and October 2008). Prior to analysis, they were combined with the ones collected from VEP in Uryu-yama in

Table 2-1 Subject plant species used for comparison of intra-leaf distribution of foliar mites between leaf morphologies. Plant species were divided by the presence (+) or absence (–) of hairs on the upper surface (U), hairs on the lower surface (L), and of leaf domatia (D). VEP samples contained only leaves from sampling periods of August 2007, June 2008, August 2008, and October 2008

Cat. of leaf morphology	Plant species (families)	Total no. of leaves
U+ L+ D+	*Viburnum erosum* var. *punctatum* (VEP) (Adoxaceae)	270
U+ L+ D–	*Rhododendron macrosepalum*, *R. obtusum* var. *kaempferi* (Ericaceae)	176
U– L+ D+	*Lyonia ovalifolia* (Ericaceae)	74
U– L+ D–	*Quercus glauca* (Fagaceae), *Pourthiaea villosa* var. *laevis* (Rosaceae), *Elaeagnus pungens* (Elaeagnaceae)	160
U– L– D+	*Acer palmatum* (Aceraceae), *Acanthopanax sciadophylloides* (Araliaceae), *Evodiopanax innovans* (Araliaceae), *Abelia serrata* (Caprifoliaceae)	278
U– L– D–	*Lindera umbellata* (Lauraceae), *Eurya japonica* (Theaceae), *Vaccinium hirtum* (Ericaceae), *Osmanthus heterophyllus* (Oleaceae)	316

the same months, which were a part of the dataset to investigate the seasonal change of mites on VEP (section 2-2-3).

Sampling was conducted during daytime but never on rainy days or on days when it had rained in the preceding 24 h. For the sampling from VEP, six leaves was collected from branches 0.5–2.0 m high of each plant, in which each leaf was taken from separate branches chosen randomly within a plant. Leaves with chlorosis symptoms were excluded from the sampling. For the sampling from the plants other than VEP, 10 (in August 2007) or six (in June 2008, August 2008, and October 2008) leaves were collected from branches 0.4–3.0 m high of each plant. Sampling from the selected non-VEP plants was conducted within 3–4 days after the VEP sampling. Each leaf was taken from separate branches chosen randomly within a plant. From *Acanthopanax sciadophylloides* Franch. et Sav. and *Evodiopanax innovans* Nakai (both Araliaceae), which possessed palmate and ternate leaves, respectively, only terminal leaflets were sampled.

Sampled leaves were immediately placed in a plastic bag, put vertically in an expanding file, and brought to the laboratory. The leaves were placed in a freezer (–10 ˚C) for >2 days before counting mites. All mites except eggs were collected and identified to the family and/or suborder level under a stereomicroscope. Sudo et al. (2010) recorded the number of mites from each leaf side (adaxial or abaxial leaf surfaces; abaxial data contained both individuals on leaf blades and inside domatia) for each plant species. Sexes and developmental stages of motile mites were not distinguished. On each plant species, mites that were expected to belong to a species newly found were mounted on microscope slides using Hoyer's medium. Sudo et al. (2010) tried to identify the specimens to the species level using the identification keys of Ehara (1980, 1993), Ehara and Gotoh (2009), and Okabe (2006). Mites for which the families or higher taxa were not determined were excluded from analyses (45 individuals from VEPs and 88 from other plants; thus, sample sizes used in this study differed from those in Sudo et al. 2010).

Eggs of Phytoseiidae and Tenuipalpidae on VEP were also counted, in addition to the motile mites. Sudo et al. (2010) attempted to identify eggs of Phytoseiidae and Tenuipalpidae according to Ehara (1993) and estimated them from the occurrence of adult individuals on the same leaf. Eggs of other mite taxa were not counted due to the difficulty of identification from external morphology.

Mite sampling method for "Seasonal change in intra-leaf distribution of mites on VEP" (2-2-3)

Samplings for VEP were conducted once a month from April to November 2007 and replicated from June to November 2008 in the same manner as described in the prior section. Over the 14 sampling periods (i.e., once a month from April to November 2007 and June to November 2008), Sudo et al. (2010) sampled leaves from 158 VEP shrubs in total for the Uryu-yama site (sample size of each period varied from 8 to 12) and from 148 VEPs in total for the Iwakura site (sample size of each period varied from 10 to 11).

2-2-2 Comparison of intra-leaf mite distribution among 15 woody plant species

Based on presence/absence of hairs and domatia, target plant species was classified into the following six categories (Table 2-1): "U+L+D+" (with hairs on both the upper and lower sides, and with leaf domatia), "U+L+D–" (hairs on upper and lower surface, no domatia), "U–L+D+" (hairs on lower side only, domatia in abaxial vein axils), "U–L+D–" (hairs only on lower surface), "U–L–D+" (no hairs, domatia present), and "U–L–D–" (no hairs, no domatia). No plants were observed with only upper-side hairs and domatia ("U+L–D+"), or with only upper-side hairs ("U+L–D–"). Hair shape and characteristics were stellate in VEP, scale in *Elaeagnus pungens* Thunb. (Elaeagnaceae), glandular trichome in *R. macrosepalum*, and short and non-glandular in the other plants. All plant species classified into any of the 'D+' classes had a bunch of hairs hanging over the vein axil, which is defined as a 'tuft'-type domatium by O'Dowd and Willson (1989), and Nishida (2004); *A. sciadophylloides* and *E. innovans* had cavities in addition to hair tufts in their vein axils, thus a mixture of tuft- and 'pocket'–type domatia (O'Dowd and Willson 1989).

For comparisons of adaxial–abaxial distribution of mites among mite taxa and/or categories of plant species with different leaf-morphology traits, log-linear models were constructed and evaluated them by both Akaike's information criterion (AIC) and the Bayesian information criterion (BIC). R version 2.10.1 (R Development Core Team 2009) and the 'loglm' module of R (in package MASS by Venables and Ripley 2002) were used for construction and selection of these models. The categories with no mites collected were regarded as sampling zeros, thus I added 0.001 to the observed frequencies of all counted data prior to model construction.

To detect the difference in intra-leaf mite distribution between plants with different leaf-surface morphology, I constructed log-linear models containing "leaf" (six categories of leaf-surface morphology), "mite" (seven distinguished mite taxa: see below), and "side" (adaxial or abaxial) as explanatory variables to explain the observed frequency (Table 2-2). Thus, the constructed log-linear model represented a 6 × 7 × 2 contingency table. Although Sudo et al. (2010) distinguished 11 mite taxa (families, superfamilies and suborders), I used the following seven categories of mite taxa for model construction: Winterschmidtiidae, Tydeoidea, Eriophyoidea, Phytoseiidae, Stigmaeidae, Oribatida, and a mixture of minor taxa (Anystidae, Cunaxidae, Tetranychidae, Tenuipalpidae, and Ixodida). I constructed nine models with all possible combinations of multi-way interactions and calculated the AIC and BIC for each combination. Data from the four sampling periods were combined prior to analysis, as the composition of identified mite taxa in fact did not change with seasons (Sudo et al. 2010).

To evaluate the effect of each categorical factor in selected models on the adaxial/abaxial distribution, R × C Fisher's exact test and subsequent pairwise Fisher's exact tests with Holm–Bonferroni correction were used.

2-2-3 Seasonal change in intra-leaf distribution of mites on VEP

To evaluate whether mite taxa and/or seasons affect the adaxial–abaxial distribution on VEP leaves, log-linear models were constructed and evaluated in the same way as the multispecies comparison mentioned above. The models contained "season" (14 months, no nest structure of duplicated months in 2 years), "mite" (nine mite taxa: see below), and "side" (adaxial or abaxial) as explanatory variables to explain the observed frequency (Table 2-3). Thus, the constructed log-linear model represented a 14 × 9 × 2 contingency table. I used the following mite taxa for model construction: Winterschmidtiidae, Tydeoidea, Eriophyoidea, Phytoseiidae, Tenuipalpidae, Tetranychidae, Oribatida, Stigmaeidae, and a mixture of minor taxa (Anystidae, Cunaxidae, and Ascidae).

The effects of each categorical factor in the selected model on the adaxial–abaxial distribution were evaluated by R × C Fisher's exact test for independence and paired Fisher's exact test with Holm–Bonferroni correction.

2-2-4 Survey on the diel dynamics of intra-leaf mite distribution on VEP

To investigate diurnal changes in the intra-leaf distribution of mites on VEP, an additional mite sampling was conducted from nine VEP shrubs in Iwakura on 31 October 2009. These shrubs were a part of the individuals used in the preceding sampling from 2007 to 2008. Sampling was conducted twice from the same plants, during the day (13:30–14:30) and at night (23:30–00:10) within a day.

Approximately 1 h before the daytime sampling, six branches were randomly chosen from each target VEP shrub, and I bound color wires on the basal parts of the branches as a mark. Each branch had at least two intact leaves. I cut out three of the six branches from each shrub with scissors at the daytime sampling; another three were cut out at the night sampling. To immobilize mites, the leaf surfaces of each branch of the shrub were immediately sprayed with an art fixative (Spray Fixative No. 600; Holbein Art Materials, Osaka) from a distance of 15 cm for 2 s, air-dried for 30 s, and then brought to the laboratory.

Mites were collected from two apical leaves on each sampled branch. Due to technical requirements, mites were counted twice. In the first inspection, I counted part of the mite population that could be recognized through semitransparent milky-white resin on the adaxial and abaxial leaf blades; I then classified them into families under the stereomicroscope (20×). These mites were removed from leaves after the first inspection. Leaves were then stirred gently in 99% acetone for 40 s and soaked for 60 s in 70% ethanol. Resin was removed by acetone treatment, but acetone hardened the lamina. Therefore, the leaves were treated with ethanol to soften them for the second inspection. After 5 min of air-drying, I re-counted mites of all motile forms on the adaxial and abaxial blades and domatia, that I was not able to find in the first inspection; they were classified

into families under the stereomicroscope (30×) and added to the first inspection samples. At the end, the number of mites that had dropped into the media (both acetone and ethanol fraction) was recorded, which were not determined by intra-leaf location and thus excluded from analyses.

The significance of diurnal difference in adaxial–abaxial distribution of each mite taxon was evaluated by Fisher's exact test.

2-3 Results

2-3-1 Comparison of intra-leaf mite distribution between plants

Sudo et al. (2010) collected 8,568 mite specimens (another 90 unidentified specimens were not included) in the abovementioned 11 mite taxa from 1,274 leaves of 15 plant species during the four sampling periods in Uryu-yama in the 2007–2008 survey, in which 8,376 mites (97.8%) (95% CI for binomial distribution: 97.4–98.1%) were collected from abaxial leaf surfaces. Four taxa – Winterschmidtiidae, Tydeoidea, Eriophyoidea, and Phytoseiidae – dominated the foliar acarine communities. For those four taxa, individuals from the abaxial leaf surfaces accounted for 99.1% (95% CI: 98.8–99.4%), 99.6% (99.3–99.7%), 79.1% (75.5–82.4%), and 93.8% (89.7–96.5%) in Winterschmidtiidae, Tydeoidea, Eriophyoidea and Phytoseiidae, respectively, and all showed

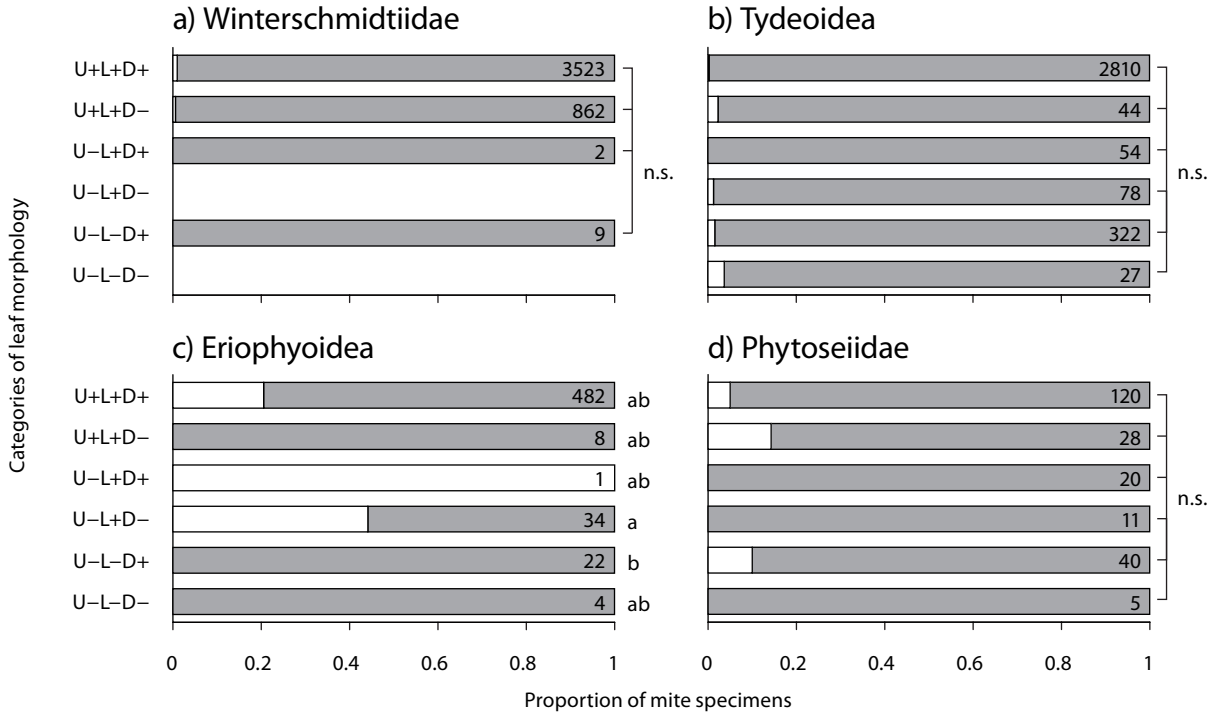

Fig. 2-1 Leaf-surface distributions of four major mite taxa on plants categorized by foliar fine structures, showing the proportions of mite individuals collected from adaxial (filled bars) and abaxial (open bars) leaf surfaces and total numbers (adaxial + abaxial) of collected mites (numerals in the bars). Unshared letters indicate a significant difference at $P < 0.05$ by 2×4 (Winterschmidtiidae) or 2×6 (other three taxa) Fisher's exact tests with Holm–Bonferroni correction. Morphology category coding is as follows: presence (+) or absence (–) of hairs on the upper (U) or lower surface (L), and of leaf domatia (D).

a significantly biased distribution (Exact binomial tests, $P < 0.001$). Of the four major mite taxa, three – Winterschmidtiidae, Tydeoidea, and Phytoseiidae – did not show any significant differences in adaxial–abaxial distribution among categories of the leaf-surface morphology (Fig. 2-1; 2 × 6 Fisher's exact test, $P > 0.05$). In contrast, the ratio of Eriophyoidea individuals collected from the adaxial side was significantly higher on U–L+D– (with only abaxial hairs, no domatia) than on U–L–D+ (no hairs, only domatia) (Fig. 2-1; Paired Fisher's exact test with Holm–Bonferroni correction, $P < 0.05$).

The saturated log-linear model, which contained all three-way and two-way interactions, was supported by AIC (i.e., the minimum value of the information criterion), whereas the model that contained two two-way interactions – "leaf × mite" and "mite × side" – was supported by the BIC (Table 2-2). The difference between the lowest AIC (saturated model) and the second lowest AIC (i.e., the model supported by the BIC) was only 2.54 (Table 2-2). This shows that only interactions of "leaf × mite" and "mite × side" are supportable. Support for "leaf × side" and the three-way interaction "leaf × mite × side" was rather marginal. Hence, it appeared that taxon composition of foliar acarine community differed with leaf surface morphology and adaxial–abaxial distribution patterns were different among mite taxa to some extent, whereas the adaxial–abaxial distribution pattern of each mite on each host plant did not differ drastically with leaf surface morphology.

Table 2-2 Multispecies log-linear models for factors "leaf" (six categories of leaf-surface morphology) and "mite" (seven distinguished taxa), that affect intra-leaf distribution of mites ("side"). Underlined figures in columns "AIC" and "BIC" signify the smallest value (i.e., the model supported by the criterion). The left side of each model formula is the observed frequency of mites

Model	*df*	X_L^2	AIC	BIC
leaf + mite + side + leaf × mite + leaf × side + mite × side + leaf × mite × side	84	0.00	<u>168.00</u>	760.69
leaf + mite + side + leaf × mite + leaf × side + mite × side	54	83.64	171.64	552.65
leaf + mite + side + leaf × side + mite × side	24	1990.79	2038.79	2208.13
leaf + mite + side + leaf × mite + mite × side	49	72.54	170.54	<u>516.28</u>
leaf + mite + side + leaf × mite + leaf × side	48	516.36	612.36	951.04
leaf + mite + side + leaf × mite	43	557.39	643.39	946.79
leaf + mite + side + leaf × side	18	2475.64	2511.64	2638.64
leaf + mite + side + mite × side	19	2031.82	2069.82	2203.88
leaf + mite + side	13	2516.66	2542.66	2634.39

2-3-2 Seasonal change in intra-leaf distribution of mites on VEP

The mite samples collected from VEP by Sudo et al. (2010) in the 2007–2008 survey were composed of 41,758 individuals (another 45 unidentified specimens were not included) belonging to the 11 different taxa (families, superfamilies and suborders) from 1,836 leaves (Fig. 2-2). Of which, 41,181 individuals (98.6%) (95% CI: 98.5–98.7%) were collected from the abaxial side of the VEP leaves. Winterschmidtiidae, Tydeoidea, Eriophyoidea, and Phytoseiidae were the four most abundant taxa, accounting for 55.9, 37.2, 3.5, and 3.0%, respectively, of all collected mites from VEP; collectively they accounted for 99.6% of all identified mite specimens. All mounted specimens of Winterschmidtiidae from VEP were *Czenspinskia lordi* Nesbitt, whereas the tydeoid and eriophyoid mites were not identified (Sudo et al. 2010). Phytoseiid mite samples consisted of *Paraphytoseius urumanus* (Ehara), *Phytoseius (Dubininellus) blakistoni* Ehara, *Phytoseius (Dubininellus) nipponicus* Ehara, *Phytoseius (Dubininellus) capitatus* Ehara, and one unknown *Phytoseius* species (Sudo et al. 2010).

Seven mite taxa were distributed in favor of the abaxial surfaces on VEP leaves, after pooling all samples from all periods at both the Uryu-yama and Iwakura sites (Fig. 2-2; exact binomial tests assuming even distribution, $P < 0.001$). As for the four dominant mite taxa mentioned above, individuals from abaxial leaf surfaces accounted for 99.5% (95% CI: 99.4–99.6%) in Winterschmidtiidae, 99.7% (99.6–99.8%) in Tydeoidea, 76.1% (73.8–78.2%) in Eriophyoidea, and 98.1% (97.2–98.8%) in Phytoseiidae. Four mite taxa did not show a significantly biased distribution; Anystidae (seven mites in total), Cunaxidae (seven), and Ascidae (only one individual was obtained

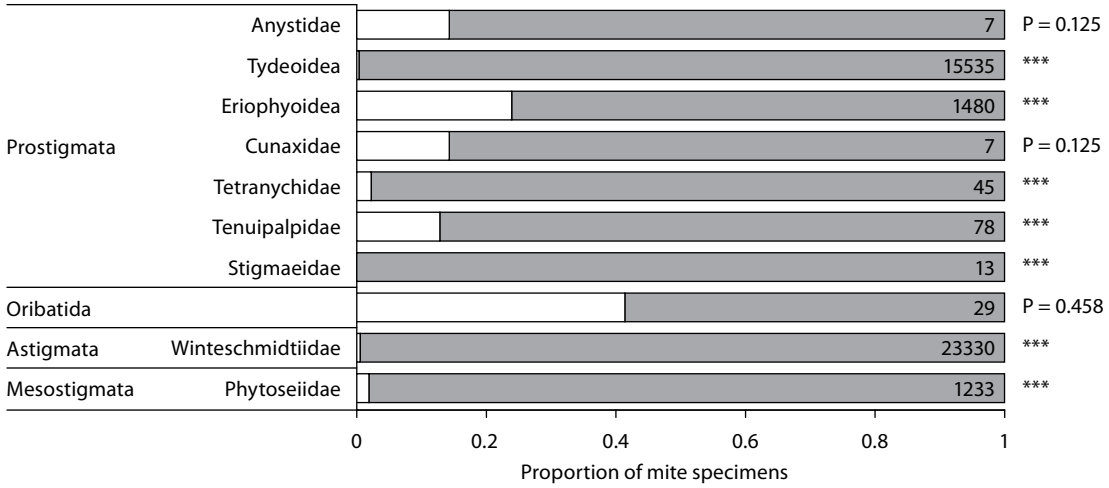

Fig. 2-2 Leaf-surface distributions of identified mite taxa on VEP showing the proportions of mite individuals collected from adaxial (open bars) and abaxial (gray bars) leaf surfaces and total numbers (adaxial + abaxial) of collected mites (numerals in the bars) in the 2-year survey at the two sites. The data on Ascidae (Mesostigmata: only one mite was found) are not shown. Asterisks shown at the right indicate significant differences (Exact binomial tests with null hypothesis of 1:1 adaxial–abaxial ratio, $P < 0.001$).

Table 2-3 Log-linear models for factors "season" (14 months) and "mite" (nine distinguished taxa), that affect the intra-leaf distribution of mites ("side") on VEP at the Uryu-yama or Iwakura sites. Underlined figures in columns "AIC" and "BIC" signify the smallest value in each site (i.e., the model supported by the criterion). Only the saturated model and supported model(s) in each site are shown. The left side of each model formula is the observed frequency of mites

Model	*df*	X_L^2	AIC	BIC
Uryu-yama				
season + mite + side + season × mite + season × side + mite × side + season × mite × side	252	0.00	504.00	2530.10
season + mite + side + season × mite + season × side + mite × side	148	112.05	<u>408.05</u>	1597.98
season + mite + side + season × mite + mite × side	135	224.90	494.90	<u>1580.31</u>
Iwakura				
season + mite + side + season × mite + season × side + mite × side + season × mite × side	252	0.00	504.00	2480.50
season + mite + side + season × mite + season × side + mite × side	148	109.39	<u>405.39</u>	<u>1566.19</u>

in the 2-year survey) were rare on VEP and tests for adaxial–abaxial distribution were not applied. Oribatid mites showed a relatively neutral distribution, more than any other mite taxa (Fig. 2-2).

At Uryu-yama, AIC supported the model with all three of the two-way interactions –"season × mite", "mite × side" and "season × side"– while the BIC supported the model that contained two two-way interactions –"season × mite" and "mite × side"– and lacked "season × side" (Table 2-3). At Iwakura, the model that contained all three of the two-way interactions was supported by both AIC and the BIC (Table 2-3). This suggests that the acarofauna on VEP changes with sampling periods (seasonal fluctuation patterns of populations differ among mite taxa), and different mite taxa on VEP have different adaxial–abaxial distributions, while the seasonal change in the adaxial–abaxial distribution of the whole foliar mite community is dependent on circumstances. Perhaps the partial support for the "season × side" interaction does not imply seasonal change of the adaxial–abaxial distribution in each mite taxon. It likely came from both of the difference in the baseline adaxial–abaxial ratios and the difference in seasonal population fluctuation patterns between mite taxa on VEP. Eriophyoidea, which has a relatively high proportion of individuals on adaxial compared to the other three major taxa, disappeared in summer while the other three taxa occurred continuously from spring to autumn.

In the four major mite taxa on VEP, three –Winterschmidtiidae, Tydeoidea, and Phytoseiidae– showed abaxial-biased distribution throughout the seasons. In 28 sample sets (14 months × 2 sites), the ratio of individuals collected from the abaxial surfaces of VEP leaves ranged from 97.1 to 99.5

to 100% (min–median–max) in Winterschmidtiidae, 97.7 to 99.7 to 100% in Tydeoidea, and 78.6 to 99.0 to 100% in Phytoseiidae. In contrast, the ratio of Eriophyoidea individuals collected from the abaxial side in each of the 12 sample sets (no eriophyoid mite was found in another 16 sample sets) ranged from 23.8 to 82.6 to 100% (min–median–max). Eriophyoid mite populations occurred twice a year; one clear peak appeared from late spring to early summer (May to July), and another peak during autumn (October and November) (Sudo et al. 2010). The ratio of eriophyoid mite individuals on adaxial leaf surfaces was significantly higher in the autumn population (6.2% in spring vs. 36.1% in autumn; Fisher's exact test, $P < 0.001$).

In Phytoseiidae, the adaxial–abaxial ratio of eggs collected from VEP leaves did not differ significantly from the ratio of the motile stage (Fisher's exact test, $P = 0.72$, n = 118 eggs; 99.2% of eggs and 98.1% of motile forms were from the abaxial side). In contrast, in Tenuipalpidae, the ratio of eggs on adaxial leaf surfaces to abaxial leaf surfaces was significantly higher than individuals at the motile stages (Fisher's exact test, $P < 0.01$, n = 62 eggs; 35% of eggs and 13% of motile forms were from the adaxial side).

2-3-3 Diel dynamics of intra-leaf mite distribution on VEP

On 31 October 2009, 540 and 303 mites were collected from 54 leaves in daytime and nighttime, respectively. Winterschmidtiidae (318 mites), Tydeoidea (237), Phytoseiidae (236), and Tenuipalpidae (41) accounted for 37.7, 28.1, 28.0, and 4.9% of all collected mite specimens, respectively, and only one eriophyoid individual was found. Another 17 mite individuals (8 winterschmidtiids, 5 phytoseiids, and 4 unidentified individuals) were found in media, and those were excluded from analyses. Numbers of mites in day and night samplings, respectively, were 237 and 81 for Winterschmidtiidae, 142 and 95 for Tydeoidea, and 121 and 115 for Phytoseiidae (Fig. 2-3).

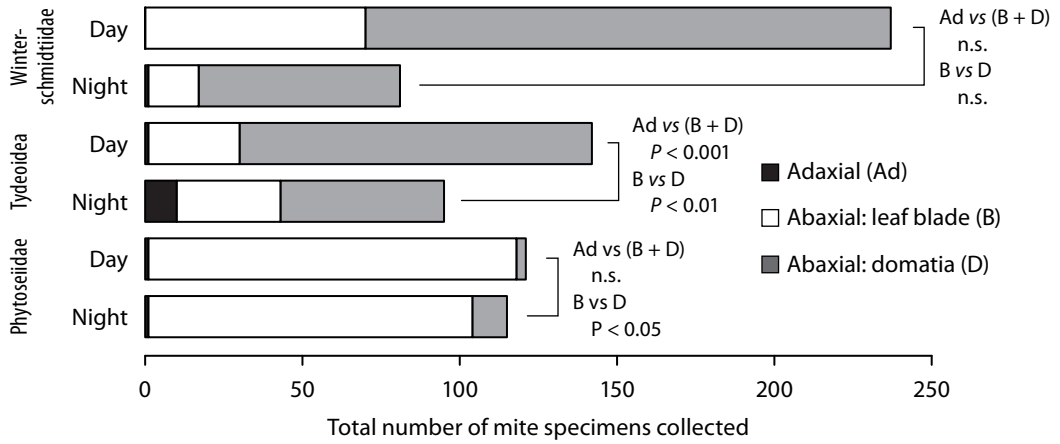

Fig. 2-3 Intra-leaf distribution of major mite taxa on VEP under day and night conditions of the sampling in Iwakura on 31 October 2009, showing the proportions of mite individuals collected from adaxial (filled bars) or abaxial (open bars) leaf blades and domatia (gray bars). P values shown at the right are by 2 × 2 Fisher's exact tests.

As for the adaxial–abaxial distribution (mite individuals from adaxial leaf surfaces vs. mites from both the abaxial leaf blades and domatia), Winterschmidtiidae and Phytoseiidae did not show diurnal change, whereas the ratio of Tydeoidea on the upper surfaces increased significantly during nighttime (Fig. 2-3). Within the abaxial side of a VEP leaf, the distribution between leaf blade and domatia changed diurnally in some mite taxa. Winterschmidtiidae did not show the diurnal difference; the ratio of tydeoid mites found inside domatia decreased at night, and the ratio of phytoseiids inside domatia increased at night (Fig. 2-3). All individuals of phytoseiids collected inside domatia were larvae or protonymphs. The adaxial–abaxial surface distributions of mites on VEP collected in Iwakura from October to November 2008 (they were collected in daytime) were 6:768 (adaxial:abaxial) for Winterschmidtiidae, 3:882 for Tydeoidea, and 2:205 for Phytoseiidae. They did not significantly differ from the 2009 daytime sampling data (0:237 for Winterschmidtiidae, 1:141 for Tydeoidea, and 1:120 for Phytoseiidae; 2 × 2 Fisher's exact tests, $P > 0.05$) (Fig. 2-3).

2-4 Discussion

Whereas the ratio of tydeoids on the adaxial leaf surfaces significantly rose at night, the majority of mites remained on abaxial leaf surface of VEP throughout seasons and this trend was consistent in daytime and night. The heterogeneity in leaf-surface morphology may explain the abaxial-biased distribution in Winterschmidtiidae, Tydeoidea and Phytoseiidae on VEP in terms of shelter and/or food availability. However, mite communities were concentrated on abaxial rather than adaxial leaf surfaces, not only on trees with dense trichomes and/or domatia but also on those with glabrous leaves, implying that the physical (i.e., abiotic) environment is a factor that accounts for the biased distribution.

Although diurnal dynamics within host plants were known in some phytoseiid mites (Onzo et al. 2003, 2009; cf. Villanueva and Childers 2005), both eggs and motile forms of phytoseiid mites were rare on adaxial surfaces in all seasons and during both day and night. Preference of mites for lower leaf surfaces had been explained as a result of adaptation to avoid wind and rainfall (Jeppson 1975). However, recent studies demonstrated that solar UVB radiation affects spider mite behavior (Ohtsuka and Osakabe 2009; Sakai and Osakabe 2010) and phytoseiid mites (Onzo et al. 2010; Tachi and Osakabe 2012), and possibly restricted their leaf surface availability.

An oribatid mite (Oribatida), the false spider mite (Tenuipalpidae: *B. obovatus*), and an eriophyid mite (Eriophyoidea) exploited not only abaxial leaf surfaces but also adaxial leaf surfaces. Oribatid mites have their center of diversity in soil ecosystems and on tree bark (Watanabe 1997; Walter and Behan-Pelletier 1999). They are characterized by armor (solid, pigmented exoskeleton) (Walter and Proctor 1999), which might work as protection against harsh environments experienced on the upper leaf surfaces.

Population density of the eriophyid mites on VEP reached peaks in spring and autumn, whereas it disappeared in summer (Sudo et al. 2010). As solar UVB radiation and temperature increases from spring to summer and decreases from summer to autumn (winter) in Japan, the occurrence of eriophyoid mites might largely depend on such physical environmental factors. In addition, the upper leaf surface is thought to offer eriophyid mites a better location than the lower leaf surface to initiate takeoff behavior for aerial dispersal because of the greater exposure to air currents (Fournier et al. 2004).

For the false spider mites (*B. obovatus*), the ratio of eggs collected from the adaxial leaf surface, to ones collected from the abaxial surface, was significantly higher than the ratio in motile individuals. *Phytoseius nipponicus* Ehara, the phytoseiid mite species commonly observed on VEP (Sudo et al. 2010) and that preyed upon *B. obovatus* eggs, is also likely to be vulnerable to UVB radiation as well as other phytoseiid mites. Oviposition on the upper leaf surfaces might provide a benefit for *B. obovatus* to decrease predation risk if their eggs are invulnerable to solar UVB radiation. The following three chapters (Chapter 3–5) concentrate on how the predator–prey interaction between *P. nipponicus* and *B. obovatus* was affected by environmental factors relevant to the upper and the lower surfaces of VEP leaves.

Chapter 3
Protective effect of stellate hairs on leaves of VEP on *Brevipalpus obovatus* eggs from the predator *Phytoseius nipponicus*

3-1 Introduction

Pubescence on plant leaves increases the abundance of sympatric phytoseiid predators of mite herbivores on the host plants (Karban et al. 1995; Loughner et al. 2008; Sudo et al. 2010). In contrast, dense hairs (trichomes) impede or delay the walking or prey searching by phytoseiid mites (Krips et al. 1999), thereby decreasing predation hazard (predation rate per unit time) on prey such as tetranychids (van Haren et al. 1987; Krips et al. 1999). The prey species of tetranychid mites appear to avoid predators by oviposition alongside leaf-surface microstructures (Krips et al. 1999; Roda et al. 2000, 2001). Hairs are generally more abundant on abaxial leaf surfaces than on adaxial leaf surfaces.

Many mites, including phytoseiid predators, preferentially inhabit lower abaxial leaf surfaces (Chapter 2). In contrast, a certain mite species such as a false spider mite *Brevipalpus obovatus* (Chapter 2) or the citrus red mite *Panonychus citri* (Jones and Parrella 1984; Fukaya et al. 2013) exploit not only lower but also upper leaf surfaces as oviposition sites. In Kyoto, *B. obovatus* occurs on VEP from late summer to mid-autumn (i.e., late August to October) during which time they coexist with phytoseiid mites, mainly *Phytoseius* spp. (Sudo et al. 2010).

VEP leaves have non-glandular stellate hairs (Chapter 2) and *B. obovatus* often lays its eggs in gaps among the hairs (Jeppson 1975; preliminary observation), on both the adaxial and abaxial leaf surfaces (Chapter 2). *Phytoseius nipponicus* preys upon *B. obovatus* eggs (preliminary observation). Some spider mite species have specific mechanisms for protecting their eggs from predators, such as spinning threads to construct complicated webs (e.g., *Tetranychus* spp.; Saito 1985) or constructing web nests and providing maternal care (e.g., *Schizotetranychus celarius* [Banks]; Saito 1986). *Brevipalpus obovatus* lacks such protection for its eggs, i.e., it produces no webbing and does not provide maternal care. Nevertheless, its egg stage lasts 9–10 days at 25°C (Goyal et al. 1985; Ehara and Gotoh 2009), which is relatively long egg duration in comparison with other spider mites.

If the stellate hairs hinder predators from accessing prey eggs, *B. obovatus* eggs might be protected from predation via the mother's oviposition site (or sides of a leaf) choice. In this chapter, whether to oviposit among hairs on VEP leaf surfaces is advantageous to *B. obovatus* from the

perspective of decreasing predation risk was tested based on sequential observations of egg production of *B. obovatus* and predation by *P. nipponicus* on the adaxial and abaxial surfaces.

3-2 Materials and methods

3-2-1 Mites

Brevipalpus obovatus was collected from wild VEP leaves in Iwakura, September 2009. The mites were reared on VEP leaf disks (abaxial surfaces) placed on water-soaked cotton in Petri dishes in a laboratory at 25°C and a 16-h light (L):8-h dark (D) cycle. The VEP leaves were also collected from Iwakura. The 40–50 day-old females (after oviposition by their mothers) of *B. obovatus*, which was potentially able to produce eggs throughout the experimental periods (Goyal et al. 1985), were used for the experiments.

Phytoseius nipponicus was collected from VEP leaves in Iwakura and reared on VEP leaf disks for 2 days before each experiment. Adults were identified in accordance with Ehara and Amano (2009), but females and males were not distinguished. Five species of Phytoseiidae have been recorded on VEP in Iwakura (Sudo et al. 2010), in which adults of *P. nipponicus* were distinguishable under a stereomicroscope (10×–50×) due to pairs of thick dorsal setae on coarse plate (Ehara and Amano 2009).

3-2-2 Host plant leaves

The VEP leaves used for the experiments were collected from four shrubs in Iwakura 2 days before each experiment. The leaves were placed with either the abaxial or adaxial side up on water-soaked cotton in Petri dishes (9 cm in diameter). Leaves that had fully developed and never been attached by leaf-chewing herbivores (leaf miners and leaf beetles) were used. The petiole of each leaf was coated with acrylic emulsion adhesive (#10824, Konishi, Osaka, Japan) to prevent the leaf surface from flooding with water. Leaves collected from the same branch were used for a batch of treatments in each replication. Before the experiments, predacious mites (Phytoseiidae and Stigmaeidae), insects (aphids, gall midges, and thrips), and rubbish (>1 mm) were removed from the leaves using tweezers. Fungivorous mites (Winterschmidtiidae and Tydeoidea), herbivorous mites (Eriophyidae), pollen, and fungi were left on the leaf surface, which functioned as food sources for *P. nipponicus* during experiments.

The leaves were photographed together with a 5-mm-diameter marker and the areas of the leaves were measured using the Histogram Function of Photoshop Elements ver. 2 (Adobe Systems Inc. 2002). The areas of the VEP leaves used in the experiment (mean ± SD) were 13.52 ± 2.55 cm^2 (adaxial, predator–), 13.35 ± 1.43 cm^2 (adaxial, predator+), 12.34 ± 3.01 cm^2 (abaxial, predator–), and 12.47 ± 3.03 cm^2 (abaxial, predator+).

3-2-3 Quantitative and qualitative comparison of stellate hairs on the surfaces of VEP leaves

To compare the stellate hairs on leaf surfaces, three leaves were collected from discrete branches from each of six VEP shrubs (18 leaves in total) in Iwakura on 24 July, 2010. The number of stellate hairs within a unit area (5 × 5 mm) was counted on the adaxial and abaxial leaf surfaces under a stereomicroscope. The unit areas were selected to be the longitudinal midpoint of the leaves, avoiding the primary vein. The number of ramifications of all stellate hairs in each unit area was also counted.

3-2-4 Effects of leaf surface and *Phytoseius nipponicus* on fecundity and egg fate of *Brevipalpus obovatus*

Eight VEP leaves were placed on water-soaked cotton in Petri dishes with the adaxial leaf surface up, and another eight leaves were placed with abaxial side up (leaf-surface treatments). The day before the experiments began (day 0), two adult *P. nipponicus* females were introduced to each of four leaves for each treatment (predator+); no phytoseiids were introduced to the remaining four leaves (predator–). Two sets of treatments (eight leaves) were set up in a plastic box (33.5 × 25 × 5 cm length × width × height) and maintained in a laboratory at 25°C (relative humidity was between 65–85%) and a 16:8 h light-dark photoperiod. The experiments were conducted in June, July, and October 2010 (4 replicates per month; 12 replicates in total).

At the beginning of the experiment (day 1), three adult *B. obovatus* females were introduced to each VEP leaf in all treatments. Over the following 10 days, the position of each newly oviposited *B. obovatus* egg was recorded every 24 h. Egg status (live or dead; died of predation or other causes) was inspected daily until its fate (hatched, preyed upon, or died of other causes) was determined. *Brevipalpus obovatus* adults were removed from leaves on day 11. If a *B. obovatus* adult escaped from a leaf disk during the 10 days, it was replaced with an adult female of the same age. The number of predators was also maintained throughout the experiment until the final egg hatchability was determined. Any *P. nipponicus* eggs were removed immediately. Larvae of *B. obovatus* were not removed throughout the experiment.

The position (contact or no contact with stellate hairs on a leaf surface) of every *B. obovatus* egg was determined under a stereomicroscope (16×). Whether the eggs were alive or dead was based on the presence or absence of egg contents and the status of the eggshell. In preliminary observations, the *B. obovatus* larva clipped the eggshell and left a round break in the eggshell when the egg hatched, while phytoseiid predators did not clip the eggshells, and no such conspicuous break was left on the eggshell when phytoseiid mites sucked the egg contents. Eggs were determined to hatch when clipping of the eggshell and disappearance of the egg contents (larva) occurred together. If the hatching of a larva was interrupted for any reason for more than 24 h, the egg was recorded as

"dead." Predation was defined as the disappearance of the egg contents in whole or in part without clipping of the eggshell. Data collection was discontinued on day 41 for the first experiment in June. In the experiments performed in July and October, observations ceased when no eggs were found to hatch after 7 consecutive days for all treatments; it was because no eggs had hatched after a 7-day no-hatching interval during the June experiments. Eggs that had not hatched by the end of the experiments were recorded as "dead."

Brevipalpus obovatus eggs that were flooded in surrounding water before hatching or predation were included only in the analyses of fecundity; they were excluded from the analyses of egg fate (hatchability or predation rates). Eggs that died from neither predation nor flooding were included only in the analysis of hatchability; they were excluded from the comparison of predation rates between leaf surfaces on each leaf.

A generalized linear mixed model (GLMM), assuming a Poisson distribution (log-link), was used to evaluate the effects of leaf surfaces and presence/absence of *P. nipponicus* on the fecundity of *B. obovatus*, in which the VEP leaves collected in each of the three months (June, July or October) were clustered. The GLMM with Poisson errors, not the analysis of variance on Gaussian ones, was used because the fecundity data did not satisfy the homogeneity of variance (Levene's test, $P < 0.001$). All combination among explanatory variables and their two-way interactions into the models were formulated, and then selected the appropriate versions based on AIC. Those models were constructed with the module "glmmML" (in the glmmML package by Broström and Holmberg 2011) of R (version 2.10.1; R Development Core Team 2009). Medians and 95th percentiles were used to represent the age distribution of *B. obovatus* eggs when they were preyed upon by *P. nipponicus* on either the adaxial or abaxial leaf surfaces; this was performed because no presupposition for age distribution at egg predation was available.

The predation hazard (i.e. the instantaneous rate of predation) for *B. obovatus* eggs of each age (day) was defined as the proportion of eggs preyed upon in the following 24 h out of the eggs that had survived each egg age. The hazard was calculated based on the egg survival data between days 2 and 11 of the experiment (i.e., the period during which *B. obovatus* adults were present). Local polynomial regression, a method of nonparametric regression, was used to represent the dynamics of predation hazard on each leaf surface. The degree of the polynomials and the span (smoothing parameter) were set at 2 and 1, respectively. For each egg, the predation rate within 24 h of oviposition was not included in the regression because of uncertainty regarding the initial number of oviposited eggs. Only the data for leaves with predators were used for the regression. The module "loess" of R ver. 2.10.1 was used for regressing predation hazards.

3-2-5 Effects of egg age on predation risk

Thirty-five VEP leaves were set with the adaxial (n = 16) or abaxial (n = 19) side up on water-soaked cotton in Petri dishes in the same manner as described above. On the first day of the experiment, three adult *B. obovatus* females were introduced to each VEP leaf. The position of every egg laid by the females was recorded every day, and the females were removed after 7 days. Then, four adult *P. nipponicus* were introduced to each leaf immediately after removing the *B. obovatus* females. The status of *B. obovatus* was checked every day for 3 days after the introduction of *P. nipponicus*.

A GLMM, assuming a binomial distribution (logit-link), was used to evaluate the effects of leaf surface and egg age on the predation rate of *B. obovatus* eggs (the proportion of eggs preyed within the 3 days after predator introduction), in which eggs laid on the same leaf were clustered. The model was constructed with the module "glmmML" of R ver. 2.10.1.

3-2-6 Effects of stellate hair manipulation on egg predation risk

A manipulative experiment was conducted to evaluate whether stellate hairs protected *B. obovatus* eggs from *P. nipponicus*. Four VEP leaves were placed on water-soaked cotton in Petri dishes with the abaxial side up. On the first day of the experiment, 10 adult *B. obovatus* females were introduced to each VEP leaf. The position of every egg laid by the females was recorded every day, and the females were removed after 3 days.

All *B. obovatus* eggs that had contact with both a vein and a stellate hair on the VEP leaf surface were studied. The eggs were divided randomly into two groups. In the first group, the eggs were moved temporarily using fine-point brushes. The stellate hairs that had direct contact with the eggs were bent at their basal parts using tweezers in order to increase the exposure of eggs touching the hairs to the predators; thus the hairs fell sideways but not removed. Then the eggs were immediately replaced to the basal part of the stellate hair (the hair-bending treatment). In the second group (control), the eggs were temporarily picked up using fine-point brushes with no modification of the stellate hairs touching eggs. Instead, a stellate hair at the second nearest neighbor of the stellate hair touching each egg was bent to imitate chemical cues for predators, if they exist.

Five adult *P. nipponicus* were introduced to each leaf immediately after removing the *B. obovatus* females. The eggs were checked every day for 3 days after the introduction of *P. nipponicus*.

3-3 Results

3-3-1 Quantitative and qualitative comparison of stellate hairs on the VEP leaf surfaces

The VEP leaves have stellate hairs on both the adaxial and abaxial surfaces, and stellate hairs and thick straight hairs also occur on the veins on the abaxial surface (Fig. 3-1ab). The adaxial leaf surfaces have more stellate hairs than the abaxial leaf surfaces, with 133.5 ± 9.34 and 104.1 ± 9.15

(mean ± SE) hairs (as hair tufts) per 5 × 5 mm area on the adaxial and abaxial surfaces, respectively (Welch's two-sample *t*-test, $t = 2.2474$, $df = 33.986$, $P < 0.05$). The mode and median for the number of ramifications of the stellate hairs were one and two on the adaxial leaf surfaces, respectively, and three and four on the abaxial leaf surfaces, indicating that the abaxial surfaces of VEP leaves have larger, more complicated stellate hairs than the adaxial leaf surfaces (Wilcoxon's rank-sum test, $W = 651855.5$, $P < 2.2 \times 10^{-16}$; Fig. 3-1c). Consequently, the abaxial leaf surfaces have more ramifications in the unit area than the adaxial leaf surfaces; 403.7 ± 44.0 and 240.5 ± 21.2 (mean ± SE) ramifications on the abaxial and adaxial surfaces, respectively (Welch's two-sample *t*-test, $t = -3.3423$, $df = 25.524$, $P < 0.01$).

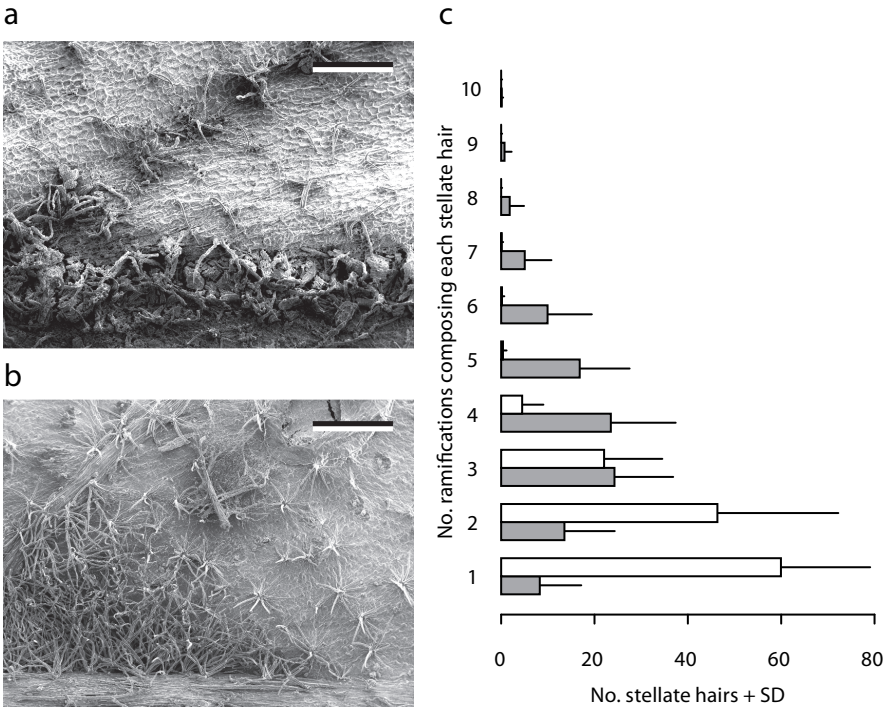

Fig. 3-1 (a, b) Stellate hairs on the surface of a VEP leaf (scanning electron microscope image), showing the (a) adaxial and (b) abaxial surfaces of the primary vein axil of the same leaf. The scale bar in each figure is 500 μm. (c) The number of ramifications of stellate hairs on the adaxial (open bars) and abaxial (gray bars) surfaces of VEP leaves as the mean frequency with the standard deviation in 18 quadrats (5 mm × 5 mm) from 18 leaves.

Table 3-1 GLMM (log-link, Poisson errors) for the fecundity of *Brevipalpus obovatus* on VEP leaves

	Coefficient	SE	z value	Pr (>|z|)
(Intercept)	2.705	0.123	22.06	0.00 ***
Surface	–0.234	0.1115	–2.100	0.0357 *
Predator	–0.468	0.1194	–3.917	8.98×10^{-5} ***
Surface: Predator	–0.328	0.1913	–1.713	0.0868

AIC = 154.6 (the selected model with two-way interaction) and 155.5 (the model without two-way interaction).

3-3-2 Effects of leaf surface and *Phytoseius nipponicus* on the fecundity and egg fate of *Brevipalpus obovatus*

Fecundity and egg fates of Brevipalpus obovatus

The fecundity of *B. obovatus* was greater on abaxial than adaxial leaf surfaces, and the presence of *P. nipponicus* reduced fecundity on both surfaces (Table 3-1). The numbers of eggs produced by three females on adaxial leaf surfaces over 10 days (mean ± SE, across the three time periods) were 12.0 ± 1.75 and 5.42 ± 0.723 in the predator– and predator+ treatments, respectively, and on the abaxial leaf surfaces 15.2 ± 3.07 and 9.50 ± 1.28. Model selection supported the GLMM containing the effect of leaf surface, predator presence and their two-way interaction, suggesting that the reduction in the fecundity of *B. obovatus* due to the presence of *P. nipponicus* was marginally mitigated on abaxial leaf surfaces compared to adaxial leaf surfaces (Table 3-1). Almost all eggs (501 of 505 eggs in total) had contact with stellate hairs on leaf surfaces.

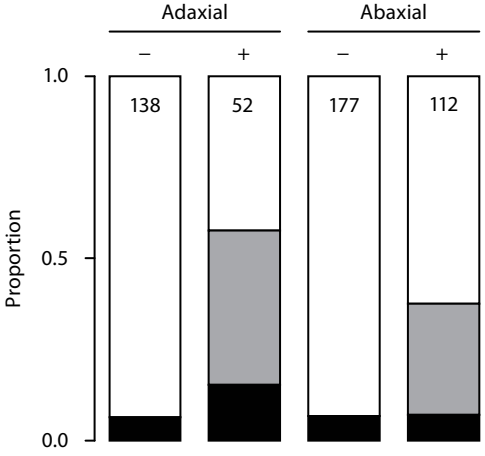

Fig. 3-2 Fate of *Brevipalpus obovatus* eggs on VEP leaves, showing the proportions of eggs that hatched (open bars), that were preyed upon (gray bars), and that died (solid bars), out of the total number of eggs (numbers in bars), in presence (+) or absence (–) of *Phytoseius nipponicus*.

On predator– leaves, most *B. obovatus* eggs hatched regardless of the leaf surface (Fig. 3-2); the hatchability was 0.935 (n = 138; 95% CI, 0.880–0.970) and 0.938 (n = 177; 95% CI, 0.891–0.969) on adaxial and abaxial leaf surfaces, respectively. On predator+ leaves, the respective hatching successes were reduced to 0.423 (n = 52; 95% CI, 0.287–0.568) and 0.634 (n = 112; 95% CI, 0.538–0.723) (Fig. 3-2). The predation rate was significantly higher on adaxial leaf surfaces (0.50; n = 44) than on abaxial leaf surfaces (0.32; n = 104) (2 × 2 Fisher's exact test, $P = 0.0418$).

Dynamics of predation risk on Brevipalpus obovatus *eggs*

Egg predation events in each experiment occurred continuously from day 3 to day 13 after the introduction of *B. obovatus* (Fig. 3-3). The eggs required 11.41 ± 0.203 and 12.02 ± 0.277 days to hatch on the leaves in the predator– and predator+ treatment groups, respectively (Fig. 3-4). Although the mechanism was unknown, the egg duration significantly elongated in the predator-present treatment than the predator-absent treatment (Wilcoxon rank sum test, $W = 11680.5$, $P = 0.02518$).

The median and 95th percentile of egg age at predation was 2.0 and 5.95 days on adaxial surfaces and 2.0 and 8.80 days on abaxial surfaces, respectively, suggesting that the predation mostly occurred in early stages of egg development (Fig. 3-4). As a result, the predation hazard for surviving

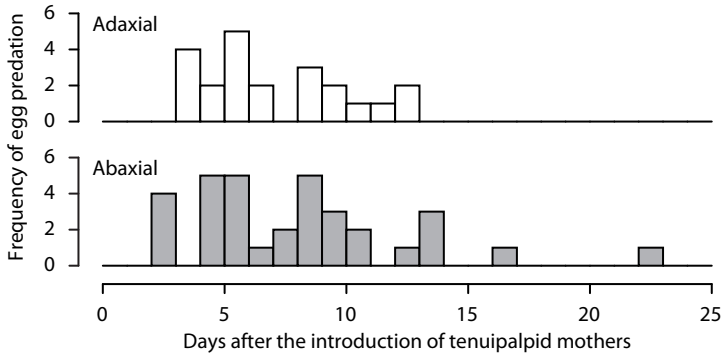

Fig. 3-3 The observed frequency of egg predation on each day since the start of the experiment (total of all replicates with predators). Bottom: abaxial leaf surfaces.

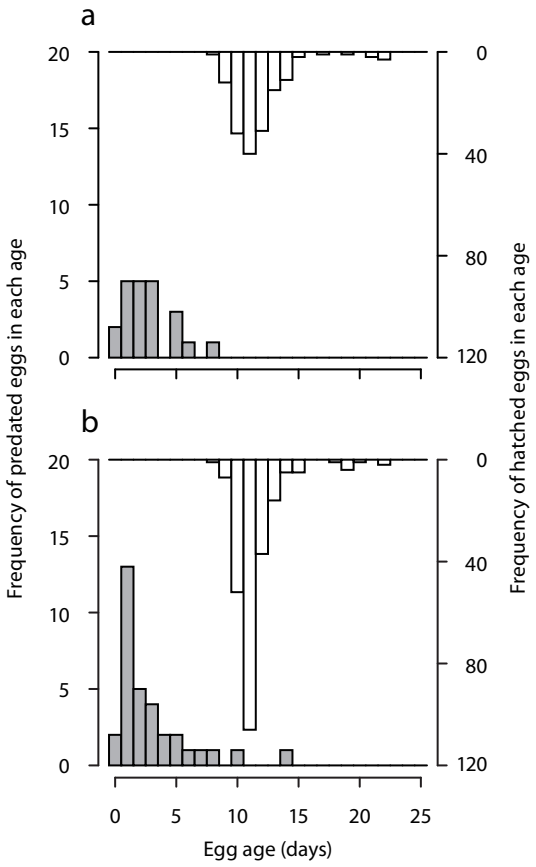

Fig. 3-4 Distribution of egg age at predation or hatching (total frequencies from all leaves with predators): (a) adaxial and (b) abaxial leaf surfaces. Gray and open bars signify preyed upon and hatched eggs, respectively.

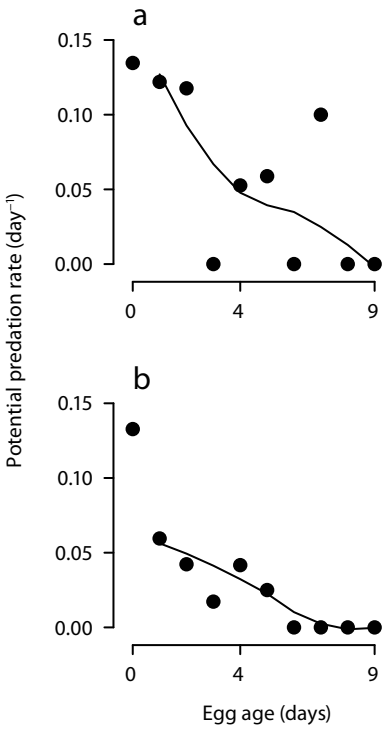

Fig. 3-5 Predation hazard per day (i.e., potential predation rate for the following 24 h) of *B. obovatus* eggs at each age (days) on (a) adaxial and (b) abaxial leaf surfaces. The hazard lines were determined using local polynomial regression (degree of polynomial = 2, span = 1.0). The predation rate within 24 h of oviposition (day zero) was not used for the regression. Only the data for leaves with predators were used.

eggs decreased with age and reached zero before the start of hatching on both adaxial and abaxial leaf surfaces (Fig. 3-5).

3-3-3 Effects of egg age on predation risk

The proportion of *B. obovatus* eggs that were preyed upon by *P. nipponicus* tended to be higher for 1- and 2-day-old eggs than older eggs, although it was as high as 0.478 for 6-day-old eggs on

Table 3-2 Predation rate (the proportion of eggs that were consumed by *P. nipponicus*) for 1- to 6-day-old *Brevipalpus obovatus* eggs on adaxial/abaxial leaf surfaces of VEP

Egg age (days)	Predation rate	
	Adaxial	Abaxial
1	0.429 (28)	0.368 (38)
2	0.486 (37)	0.410 (39)
3	0.314 (35)	0.258 (31)
4	0.286 (35)	0.306 (26)
5	0.353 (34)	0.267 (30)
6	0.478 (23)	0.227 (22)

The numbers in parentheses are the numbers of eggs tested.

the adaxial leaf surfaces (Table 3-2). Overall, the predation rate on the adaxial surface (0.379; n = 195; 95% CI, 0.311–0.452) tended to be higher than that on the abaxial surface (0.312; n = 199; 95% CI, 0.248–0.381). However, the model selection rejected the effects of both leaf surface and egg age on egg predation rate (binomial GLMM, logit-link); the AICs were 486.72, 487.63, and 488.17 in the null model, the model containing "age," and the model containing "surface," respectively. Consequently, the effects of egg age and leaf surface on predation risk were not proven.

3-3-4 Effects of stellate hair manipulation on egg predation risk

The proportion of *B. obovatus* eggs consumed by *P. nipponicus* over 3 days was 0.94 (n = 47; 95% binomial CI, 0.82–0.99) for eggs attached to bent stellate hairs and 0.64 for eggs attached to normal stellate hairs (control; n = 45; 95% CI, 0.49–0.78). The difference in egg consumption by the hair-bending treatment was significant (Fisher's exact test, $P < 0.001$), indicating that the stellate hairs of VEP leaves reduce the predation risk of *B. obovatus* eggs by *P. nipponicus*.

3-4 Discussion

Brevipalpus obovatus eggs that survived for more than 6 days (approximately half of their incubation periods observed in this experiment) were scarcely preyed by *P. nipponicus*. *Phytoseius nipponicus* constantly preyed on *B. obovatus* eggs while *B. obovatus* females produced new eggs, suggesting that some particular factor other than the activity of *P. nipponicus* reduced risk of aged *B. obovatus* eggs being preyed. Possible mechanisms reducing the predation risk during the late egg period of *B. obovatus* include augmentation of the egg defense system itself, such as physical and chemical defense, and the hindering effects of stellate hairs. However, there was no obvious effect of the age

of eggs on the reduction of predation risk during the late egg period. Instead, a protective effect of stellate hairs on *B. obovatus* eggs hindering predation by *P. nipponicus* was directly demonstrated in the manipulative experiments.

Literatures reported that the walking and foraging capacities of phytoseiid mites are determined by the interaction between the trichome density on the leaf surface and body width of the phytoseiid mites (Krips et al. 1999; Kreiter et al. 2002). The body length and width of *B. obovatus* adult females are 290 and 170 μm, respectively (Ehara and Gotoh 2009), while those of *P. nipponicus* are 360 and 230 μm, respectively (Ehara 1962). At oviposition sites, *B. obovatus* may be able to exploit gaps that are narrower than the minimum gap size that *P. nipponicus* can enter. Therefore, a reduction in the predation rate with egg age should result as the accessible eggs are removed from the leaf surfaces by predation, making it more difficult for the predators to find the remaining (older) eggs.

Phytoseius nipponicus may have more difficulty penetrating *B. obovatus* eggs laid among the dense stellate hairs on the abaxial surfaces of VEP leaves than on the adaxial. Stellate hairs on the abaxial surfaces of VEP leaves had more ramifications than ones on the adaxial surfaces. Consequently, more eggs survived on the abaxial than on the adaxial surfaces after the whole incubation periods with predators, suggesting that stellate hairs on abaxial leaf surfaces of VEP protected *B. obovatus* eggs more effectively than on the abaxial. Additionally, *B. obovatus* eggs under stellate hairs on VEP leaves considerably survived also on adaxial surfaces of VEP leaves. These are the evidence that stellate hairs protect *B. obovatus* eggs from *P. nipponicus*. The oviposition-site choice in *B. obovatus* laying most eggs in contact with the stellate hairs is beneficial in reducing predation risk on eggs. Whether or how an adult *B. obovatus* assess the accessibility of a phytoseiid predator to each oviposition site (e.g. the width of the gap between stellate hairs) is an interesting issue from an biological point of view.

Although the protective function of the leaf surface microstructure was greater on abaxial leaf surfaces, a substantial portion of *B. obovatus* eggs (35%) and motile individuals (13%) remained on the adaxial leaf surfaces of VEP. On the other hand, whereas only 1.9% of the phytoseiid mite population was found on the adaxial leaf surfaces (Chapter 2). In the next chapter, I address the geotaxis and the leaf-surface preferences of *B. obovatus* and *P. nipponicus*, which might lead to a spatial segregation and change in the interaction between the predator and the prey on VEP plants, in comparison with a leaf disk.

Chapter 4
Habitat segregation caused by opposite geotaxis and leaf-surface preferences mitigates negative effects of *Phytoseius nipponicus* on *Brevipalpus obovatus*

4-1 Introduction

Hairs and/or trichomes that obstruct prey searching and predation by phytoseiid mites (Krips et al. 1999; Loughner et al. 2010) are generally denser and better developed on abaxial than on adaxial leaf surfaces (Chien and Sussex 1996). Accordingly, predation efficiency may be greater on the adaxial sides of leaves. Using leaf disks as test substrata, more eggs of an herbivorous false spider mite, *Brevipalpus obovatus*, were consumed by the predator *Phytoseius nipponicus* on adaxial than on abaxial surfaces of VEP (Chapter 3). The protective function of the leaf surface microstructure was greater on the abaxial leaf surfaces of VEP (Chapter 3), suggesting that oviposition on the adaxial leaf surfaces is detrimental for *B. obovatus* in the face of predation risk from *P. nipponicus*. Nevertheless, a substantial portion of *B. obovatus* eggs (35%) and motile individuals (13%) remained on the adaxial leaf surfaces of wild VEP (Chapter 2).

At the same time, 98% of the phytoseiid mite population was found on the abaxial (i.e., lower) leaf surfaces of VEP (Chapter 2). If the occurrences on upper and lower leaf surfaces are mismatched between the prey and the predator, such a difference in spatial distribution might mitigate predation risk on *B. obovatus* eggs. Phytoseiid mites in the genus *Phytoseius*, which occur dominantly on VEP leaves, are generalist predators that depend on a range of alternative food sources (McMurtry and Croft 1997). Because the prey–predator relationship between *B. obovatus* and *P. nipponicus* is not specific, it may not have a role in leaf-surface choices in prey populations. However, if upper leaf-surface exploitation mitigates predation risk, *B. obovatus* should respond behaviorally to the presence of *P. nipponicus*.

In this chapter, I investigated the factors that affect leaf-surface distribution and tested whether the presence of *P. nipponicus* alters the leaf-surface distribution and reproductive success of *B. obovatus*. VEP leaves were used as substrata and deployed devices that made both surfaces accessible to the mites; they were set in natural and inverted (upside down) positions to explore the effects of

gravity and heterogeneous microstructure (density of leaf hairs) of leaf surfaces on intra-leaf distributions of the prey–predator system.

4-2 Materials and methods

4-2-1 Mites

I collected *B. obovatus* occurring on VEP leaves in Iwakura, September 2009. The mites were reared on VEP leaf disks (abaxial surfaces) placed on water-soaked cotton in Petri dishes in a laboratory at 25°C and a 16-h light (L):8-h dark (D) cycle. I used *B. obovatus* females that were 40–50 days old (measured as the duration of time since the mothers had oviposited the eggs from which they hatched).

Phytoseius nipponicus, a generalist phytoseiid species that is predominant in the foliar mite community on VEP in Kyoto (Sudo et al. 2010), was collected from VEP leaves in Iwakura and reared on VEP leaf disks for 2 days prior to experiments. *Phytoseius nipponicus* adults (both females and males) were identified by pairs of thick dorsal setae on the coarse plate (Ehara and Gotoh 2009).

4-2-2 Host-plant leaves

I collected VEP leaves from four shrubs in Iwakura 2 days before each experiment. Leaves were assembled into experimental configurations within 6 hours of collection. Predacious mites (Phytoseiidae and Stigmaeidae), insects (aphids, gall midges, and thrips), and debris (>1 mm) were removed from the leaves prior to the experiments. Fungivorous mites, herbivorous mites (Eriophyoidea), pollen, and fungi were left on leaf surfaces.

4-2-3 Experimental setups

To explore how mites use upper/lower or adaxial/abaxial surfaces, VEP leaves were held in a plastic frame (leaf holder: LH; 29.4 × 8.4 × 3.0 cm; Fig. 4-1) that permitted changes in leaf orientation. Two VEP leaves were held in a LH, and the basal halves of both leaf blades were wrapped in cotton fabric (15 × 7 cm). The cotton fabric was fastened onto the frame with adhesive tape (Mask Light Tape #730, Sekisui Chemical, Osaka). Of the two leaves held on a single LH, one was set with the adaxial surface upward (TRUE gravity) and the other with the abaxial surface upward (INVERTED gravity). To prevent leaves from flooding with water, acrylic emulsion adhesive (#10824, Konishi, Osaka) was painted where the leaf blade met the cotton fabric (Fig. 4-1). To prevent mites escaping, leaf surfaces were coated 4 mm distant from the cotton fabric with sticky grease (Tangle B grease; Fuji Yakuhin Kogyo, Tokyo). Available leaf spaces (distal part of the leaf blade measured from the boundary of the sticky grease) were 10.52 ± 6.12 cm^2 (mean ± SD per leaf surface), 9.60 ± 2.89 cm^2, 8.62 ± 1.82 cm^2, and 9.34 ± 2.32 cm^2 in the TRUE-gravity configuration

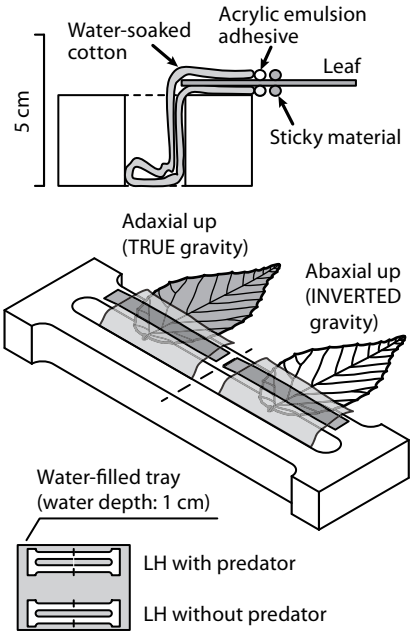

Fig. 4-1 Leaf holder (LH) used to test the intra-leaf distribution of mites.

without predators, TRUE-gravity configuration with predators, INVERTED-gravity configuration without predators, and INVERTED-gravity configuration with predator treatments, respectively. Areas were measured with the Histogram Function of Photoshop Elements ver. 2 software (Adobe Systems, San Jose, CA, USA).

Two LHs (bearing four leaves in total) were placed in rectangular plastic tray (33.5 × 25 × 5 cm) containing distilled water 1 cm deep. Leaves held in the LHs were supplied with water via the cotton fabric. LHs were maintained on a laboratory shelf at 25°C under a L16:D8-h photoperiod. LHs were illuminated with 40 W fluorescent lamps fixed at 40-cm intervals on a sidewall 30 cm distant from the shelf. I used a crossed design with predators (absent/present) and gravity (TRUE/INVERTED) as independent variables. Two LHs in a single tray were used as duplicates, and leaves collected from the same branch were used as replicates.

4-2-4 Experimental design

A two-way factorial design was used in August, October, and November 2010. In each experimental period, I prepared four trays containing two LHs (eight LHs in total). Each tray contained a series of VEP leaves assigned to (1) predator-absent TRUE-gravity, (2) predator-absent INVERTED-gravity, (3) predator-present TRUE-gravity, (4) predator-present INVERTED-gravity treatments.

The day before the beginning of experiment (day 0), I introduced three adult *P. nipponicus* onto each of the two leaves held in one LH (predator-present TRUE/INVERTED-gravity) assembly but not onto the other LH (predator-absent TRUE/INVERTED-gravity) in the same tray. The following day (day 1), three adult *B. obovatus* females were introduced onto all VEP leaves in the four trays. At daily intervals over the next 10 days (days 2–11), I recorded leaf-surface distributions of mite adults (*P. nipponicus* and *B. obovatus*) on each VEP leaf. I first counted the mite adults on the upper sides (whether adaxial or abaxial) of the leaves on each LH using a stereomicroscope with 13× magnification; I then turned over the LH and immediately counted mites on the lower sides of leaves. Introduced *B. obovatus* females were removed from the leaves on day 11. If *B. obovatus* females had escaped from the leaves before day 10, they were compensated by adding fresh female conspecifics of the same age. If the number of *P. nipponicus* mites had decreased, I added

fresh individuals every day until the egg hatchability of *B. obovatus* had been determined. Eggs of *P. nipponicus* were removed from the leaves immediately after I found them.

The locations of newly-laid *B. obovatus* eggs on the leaves were recorded every 24 hours. Subsequently, all eggs were inspected daily until the fate of each egg had been identified as (i) hatched, (ii) lost to predation, or (iii) lost to other causes. Egg vitality was assessed in the same manner as described in Chapter 3-2-4.

In the first experiment that was set up in August 2010, the observation of *B. obovatus* eggs was continued until day 41. It was beyond the maximum incubation period of *B. obovatus* eggs at the room temperature of 25°C (22 days), which I had determined in the preceding experiments in Chapter 3. During the August experiment, no egg had hatched after a 7-day interval since the last hatching. Therefore, in October and November, observations were discontinued if no eggs had hatched during the previous 7 days across all treatments. I categorized eggs that had not hatched by the end of the observation as dead.

Six leaves withered before the experiments were completed. Thus, I used data collected from 10 leaves in the predator-absent TRUE-gravity and predator-present INVERTED-gravity treatments; data were collected from 11 leaves in the predator-present TRUE-gravity and predator-absent INVERTED-gravity treatments.

4-2-5 Data analyses

Brevipalpus obovatus eggs that were flooded before hatching or predation (48 of 944 eggs in total) were excluded from egg-fate categorization. Eggs died of factors other than predation and flooding were included in analyses of hatchability but excluded from comparisons of predation rates between leaf surfaces.

I constructed GLMMs and generalized linear models (GLMs) using modules "glmmML" (in package glmmML by Broström and Holmberg 2011) and "glm" of R version 2.10.1 (R Development Core Team 2009), respectively. We calculated 95% confidence intervals (95% CI) for rates based on the binomial distribution.

Effects of gravity direction and leaf surface on intra-leaf distribution of the predator and Brevipalpus obovatus *adults*

GLMMs assuming the binomial distribution (logit-link) were used to evaluate (i) the effects of gravity direction (TRUE/INVERTED) on intra-leaf distribution (lower/upper side of leaves) of *P. nipponicus* adults and (ii) the effects of gravity direction and predator (absence/presence of *P. nipponicus*) on the intra-leaf distribution of *B. obovatus* adults. Because the counting was repeated 10 times (separate days) on every leaf, leaves were assigned random-effect status in mixed modeling to prevent pseudo-replication. I formulated all combinations among explanatory variables and their two-way interactions into the models, and then selected the appropriate versions based on AIC.

Avoidance of predator-abundant leaf surfaces by Brevipalpus obovatus *females*

The predator-present INVERTED-gravity treatments explored the effects of predator frequency on upper/lower distribution of *B. obovatus* females; this test evaluated whether *B. obovatus* females avoided leaf surfaces with abundant predators. The cumulative number of predators (explanatory variable) and *B. obovatus* females (response variable) on upper and lower leaf sides were used in a GLM analysis assuming binomial distribution (logit-link) following a Wald test.

Indirect effects of predators on fecundity of Brevipalpus obovatus

To explore the effects of predator and gravity direction on the fecundity of *B. obovatus*, I used the total number of eggs laid on a single leaf during the first 10 days (days 2–11) as the subject variable for GLM analysis, assuming a Poisson distribution (log-link); suitable model was then selected by their AICs.

Factors affecting oviposition-site choice by Brevipalpus obovatus

To determine factors affecting oviposition-site (leaf surface) choice by *B. obovatus*, I formulated all combinations among surface (leaf surface: adaxial/abaxial), side (direction of leaf surface facing: lower/upper), predator, and their interactions into the GLMMs (log-link, Poisson error) and then selected those with the lowest AIC values. Total fecundity over 10 days on each leaf surface was used as the subject variable; it was offset by the cumulative observed frequency of *B. obovatus* mothers on the surface over 10 days. The data obtained from the two surfaces of an identical leaf were clustered for mixed modeling.

Effects of leaf surfaces and direction of gravity on Brevipalpus obovatus *egg hatchability*

I used GLMMs (logit-link, binomial error) and model selection by AIC value to explore effects of gravity direction and side on egg predation (preyed upon or not based on individual *B. obovatus* eggs) in the predator-present treatments. Eggs laid on the same leaf were clustered for mixed modeling.

4-3 Results

4-3-1 Effects of direction of gravity and leaf surface on intra-leaf distribution of *Phytoseius nipponicus* and *Brevipalpus obovatus* adults

Median frequencies of *P. nipponicus* adults on upper sides (leaf surface facing upward) of VEP leaves were 16.7 and 54.4% in TRUE (adaxial leaf surfaces) and INVERTED (abaxial leaf surfaces) gravity treatments, respectively (Fig. 4-2). The model selection supported a version containing gravity direction as an explanatory variable for the intra-leaf distribution of *P. nipponicus* adults (Table 4-1). The coefficient of intercept was negative, whereas the coefficient of gravity direction (INVERSE) was positive, but it did not override the effect of the intercept. Consequently, *P. nip-*

Table 4-1 GLMM (logit-link, binomial error) for leaf-surface distribution (upper versus lower surface) of *P. nipponicus* adults. AIC = 271.0 (the selected model) or 287.5 (model with intercept only)

	Coefficient	SE	z value	Pr (>|z|)
(Intercept)	–1.535	0.196	–7.828	5.00×10^{-15}
Gravity direction (INVERSE)	1.358	0.258	5.269	1.37×10^{-7}

Table 4-2 GLMM (logit-link, binomial error) for leaf-surface distribution (upper versus lower surface) of *B. obovatus* adults. AIC = 557.6 (the selected model) or 558.7 (second lowest AIC value: model lacking the interaction term)

	Coefficient	SE	z value	Pr (>|z|)
(Intercept)	0.546	0.294	1.859	0.063
Gravity direction (INVERSE)	–0.681	0.405	–1.682	0.093
Predator (present)	0.247	0.407	0.607	0.544
Gravity direction (INVERSE): predator (present)	–1.040	0.576	–1.805	0.071

Table 4-3 Binomial GLM (logit-link) for the effect of predator distribution on leaf-surface distribution (upper surface versus lower) of *B. obovatus* adults in predator-present INVERTED-gravity treatments. The explanatory variable of the model is the total observed frequency of *P. nipponicus* on the upper side of each VEP leaf over 10 days

	Coefficient	SE	z value	Pr (>|z|)
(Intercept)	0.285	0.391	0.728	0.467
Predator frequency on the upper side	–0.129	0.047	–2.740	0.006

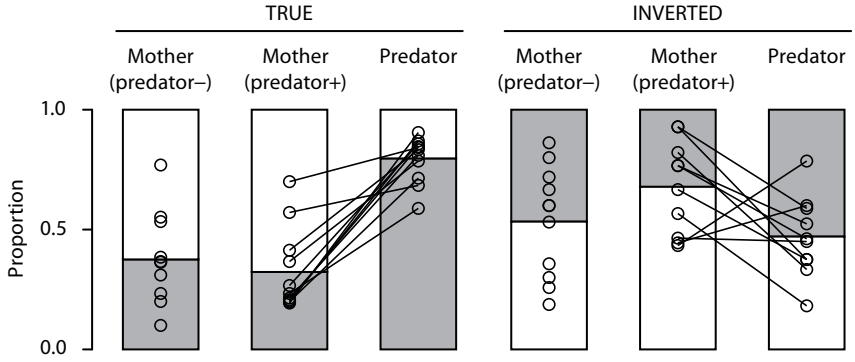

Fig. 4-2 Distribution of mite adults on VEP leaves, showing proportions of individuals on upper and lower sides of leaves (total frequency through the first 10 days of the experiment). Open and gray bars indicate proportions of mites on adaxial and abaxial leaf surfaces, respectively. Each circle in the bars signifies the distribution of mites on each leaf, and the segments between circles in "Mother (predator+)" and "Predator" indicate that data came from same leaf.

ponicus adults prefer the lower sides to the upper sides of VEP leaves (i.e., these mites have positive geotaxis) and tend to favor abaxial over adaxial leaf surfaces.

In predator-absent treatments, medians of *B. obovatus* adult frequencies on the upper sides of VEP leaves were 63.5 and 40.0% in the TRUE- and INVERTED-gravity treatments, respectively (Fig. 4-2). In the predator-present treatments, these medians changed to 76.7 and 28.3% in the TRUE- and INVERTED-gravity treatments, respectively. Model selection for the intra-leaf distribution of *B. obovatus* adults supported a version containing gravity direction, predator (absence/presence), and their interaction term as explanatory variables (Table 4-2). The coefficient of the intercept was positive, whereas the coefficient of gravity direction was negative, overriding the effect of the intercept, indicating a preference for adaxial over abaxial surfaces and for the upper over the lower side of VEP leaves (i.e., negative geotaxis) in *B. obovatus* females. The positive coefficient of predator and the negative coefficient of the interaction term (gravity direction × predator) indicate that the presence of *P. nipponicus* motivates *B. obovatus* females to move to adaxial leaf surfaces (Table 4-2).

4-3-2 Avoidance of predator-abundant leaf surfaces by *Brevipalpus obovatus*

Although *P. nipponicus* adults were concentrated on lower sides of VEP leaves under the TRUE-gravity configuration, the distribution of predators was divided between upper and lower sides on inverted leaves (Fig. 4-2). GLM analysis followed by Wald testing demonstrated that *P. nipponicus* frequency had negative effects on the frequency of *B. obovatus* females present on the same leaf side; the coefficient was −0.12942 (Table 4-3). *Brevipalpus obovatus* females actively avoided predator-abundant leaf sides regardless of leaf surface type (adaxial/abaxial).

4-3-3 Indirect effects of predators on the fecundity of *Brevipalpus obovatus*

The numbers of eggs per leaf laid by three *B. obovatus* females over 10 days were 24.0 ± 3.31 (mean ± SE), 21.1 ± 2.64, 24.6 ± 2.86, and 20.1 ± 3.05 in the predator-absent TRUE-gravity, the predator-present TRUE-gravity the predator-absent INVERTED-gravity and the predator-present INVERTED-gravity treatments, respectively. Model selection supported the GLM containing only predator (AIC = 360.8) as an explanatory variable over a version containing both gravity direction and predator but lacking the interaction term (the second lowest AIC: AIC = 362.8). The fecundity of *B. obovatus* on both leaf surfaces was reduced by the presence of predators (indirect effects) regardless of the gravity direction.

4-3-4 Factors affecting oviposition site choice by *Brevipalpus obovatus*

Distribution of *B. obovatus* eggs was obviously biased toward adaxial leaf surfaces (Fig. 4-3), and the upper side was preferred over the lower as an oviposition site. The proportion of eggs laid on

adaxial surfaces was 0.704 (n = 240, 95% CI: 0.642–0.761) in the predator-absent TRUE-gravity treatments, 0.677 (n = 232, 95% CI: 0.612–0.736) in the predator-present TRUE-gravity treatments, 0.518 (n = 272, 95% CI: 0.457–0.579) in the predator-absent INVERTED-gravity treatments, and 0.610 (n = 200, 95% CI: 0.539–0.678) in the predator-present INVERTED-gravity treatments. Though these distributions of eggs (Fig. 4-3) resembled the upper–lower frequency ratios of *B. obovatus* mothers (Fig. 4-2), environmental factors also affected the egg-production rate in individual females. Poisson GLMMs and subsequent model selection supported the selection of side, surface, predator, and the two-way surface × predator interaction as explanatory variables for 10-day fecundity on the two leaf surfaces offset by observed frequencies of *B. obovatus* mothers (Table 4-4). When *P. nipponicus* was absent, the coefficients of the models when mothers were on the leaf sides facing upward were 0.123 units higher than coefficients for models when mothers were on surfaces facing downward (signifying a fecundity increase of 13% in the natural logarithm-linked model). When mothers were on adaxial surfaces, coefficients were 0.102 units higher than when they were on abaxial surfaces (an increase of 11%). On the adaxial leaf surfaces, the introduction of *P. nipponicus* decreased fecundity by 0.233 units (a decrease of 21%). In contrast, the presence of predators scarcely affected fecundity (0.009 units; 1% increase) on abaxial surfaces.

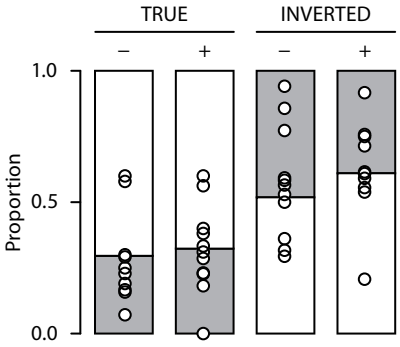

Fig. 4-3 Distributions of *B. obovatus* eggs on leaves in the predator-absent/present TRUE/INVERTED-gravity treatments. Open bars indicate the proportions of eggs oviposited on adaxial surfaces, and gray bars indicate proportions on abaxial sides. Minus and plus signs above the bars indicate predator-absent and predator-present treatments, respectively. Circles in the bars represent the proportions of eggs laid on the lower surfaces of each leaf.

Table 4-4 GLMM (log-link, Poisson error) for 10-day fecundity of *B. obovatus* on each surface of VEP leaves offset by the observed frequencies of the mothers on each surface. AIC = 180.9 (the selected model) and 181.7 (the second lowest AIC value: model lacking the surface × predator interaction term)

	Coefficient	SE	z value	Pr (>|z|)
(Intercept)	–0.392	0.118	–3.334	8.57×10^{-4}
Side (upward)	0.123	0.071	1.738	0.082
Surface (adaxial)	0.102	0.098	1.048	0.295
Predator (present)	0.009	0.158	0.059	0.953
Surface (adaxial): predator (present)	–0.243	0.144	–1.686	0.092

Table 4-5 GLMM (logit-link, binomial error) of predation risk (preyed upon vs. not preyed upon) for each *B. obovatus* egg on a VEP leaf with the predator. Eggs that died (but were not preyed upon) were excluded from the analysis. AIC = 531.1 (the selected model) and 532.9 (second lowest model, which contains the interaction term)

	Coefficient	SE	z value	Pr (>|z|)
(Intercept)	0.252	0.318	0.794	0.427
Side (upper)	−0.491	0.236	−2.084	0.037
Gravity direction (INVERSE)	−0.664	0.413	−1.608	0.108

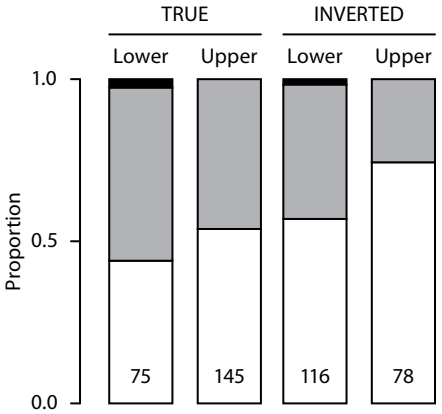

Fig. 4-4 Proportion of *B. obovatus* eggs that hatched (open bars), died from predation (gray bars), and died due to other factors (filled bars) on upper and lower surfaces of VEP leaves in the predator-present TRUE- and INVERTED-gravity treatments. Numbers in the bars are total numbers of eggs observed in each treatment.

4-3-5 Effects of leaf surfaces and direction of gravity on *Brevipalpus obovatus* egg hatchability

When predators were absent, almost all *B. obovatus* eggs hatched regardless of leaf surface. In predator-absent TRUE-gravity treatments, the hatchability ratios were 0.975 (n = 159, 95% CI: 0.937–0.993) and 0.943 (n = 70, 95% CI: 0.860–0.984) on adaxial (upper) and abaxial (lower) leaf surfaces, respectively. In predator-absent INVERTED-gravity treatments, hatchability was 1.000 (n = 129, 95% CI: 0.972–1.000) and 0.984 (n = 124, 95% CI: 0.943–0.998) on abaxial (upper) and adaxial (lower) leaf surfaces, respectively.

However, egg hatchability decreased in the presence of predators, and the magnitude of the reduction was greater on the lower sides of leaves (Fig. 4-4). In predator-present TRUE-gravity treatments, hatchability was 0.538 (n = 145, 95% CI: 0.453–0.621) and 0.440 (n = 75, 95% CI: 0.325–0.559) on upper (adaxial) and lower (abaxial) sides of leaves, respectively. In the predator-present INVERTED-gravity treatments, hatchability was 0.744 (n = 78, 95% CI: 0.632–0.836) and 0.569 (n = 116, 95% CI: 0.474–0.661) on upper (abaxial) and lower (adaxial) sides of leaves, respectively. The model selection supported the selection of gravity direction (TRUE/INVERTED) and side (upper/lower) as explanatory variables for egg predation risk (Table 4-5). This indicates that predation rate was lower on the upper than on the lower sides of VEP leaves; the INVERTED-gravity treatment moderated the risk of predation by *P. nipponicus* for *B. obovatus* eggs.

Most *P. nipponicus* predation on individual *B. obovatus* eggs occurred within the first half of the egg period. The mean incubation period for *B. obovatus* eggs was 11.66 days, and this was unaffected by gravity direction, leaf surface (adaxial or abaxial), and absence/presence of predators (Poisson GLMM analysis with log-link). The 95th percentiles of ages of eggs eaten by the predator were 5.7 and 6 days on predator-present leaves with TRUE- or INVERTED-gravity treatments, respectively.

4-4 Discussion

Abaxial surfaces of VEP leaves have more stellate hairs than adaxial surface. Dense leaf hairs on the abaxial surface protect eggs of *B. obovatus* from *P. nipponicus* predation more effectively than ones on the adaxial (Chapter 3). Nevertheless, *B. obovatus* adults occur more frequently and oviposit more often on adaxial leaf surfaces than on the obverse surfaces. This contradicting behavior was explained by the effects of gravity and leaf-surface architecture on local predator density. Positive geotaxis and a preference for abaxial surface accounted for the concentration of *P. nipponicus* population on lower abaxial leaf surfaces. Conversely, negative geotaxis and a preference for adaxial surface over the abaxial surface drove *B. obovatus* to upper adaxial leaf surfaces. Such combination between the direction of gravity pull and leaf-surface architecture explain the occurrences of *P. nipponicus* and *B. obovatus* on different surfaces of the same leaf. This spatial segregation reduces opportunities for encounters between predator and prey.

The daily fecundity of *B. obovatus* on predator-present leaves was ≈5/6 that on predator-free leaves. This reduction was interpreted as an indirect negative effect of predator presence. A greater reduction in fecundity was observed in the experiments using VEP leaf disks (Chapter 3: where three *B. obovatus* mothers versus two predators per leaf disk). Oviposition rates of *B. obovatus* on adaxial and abaxial leaf surfaces decreased to 1/2 and 2/3 in the presence of predators, respectively, in comparison with predator-free surfaces. In addition to having reversed preferences for gravity direction and leaf surfaces in comparison with *P. nipponicus*, *B. obovatus* adults actively changed their leaf-surface distribution to avoid the predator. This change in distribution probably mitigated the decrease in *B. obovatus* fecundity when both leaf surfaces were available.

The egg-predation rate was lower on the upper sides of VEP leaves than on the lower sides. Reduced predation risk may compensate for the reduced frequency of sheltered sites for oviposition on the upper adaxial surface of a VEP leaf (Chapter 3). Effects of leaf-surface microstructures (e.g., hairs, glandular trichomes, and domatia) on loss rates of plant mites and their eggs to predation have been investigated previously (e.g. van Haren et al. 1987; Krips et al. 1999; Norton et al. 2001; Roda et al. 2001), but the effects of leaf side (upper or lower) were scarcely considered in the past. In this chapter it was revealed that gravity direction affected prey–predator interactions in a foliar mite community, between *B. obovatus* and *P. nipponicus*.

In many mite herbivores, eggs were laid on the upper leaf surfaces of their host plants, only when population densities reach a saturation point on lower-leaf surface (Jeppson 1975). However, the oviposition rate of *B. obovatus* was slightly higher on the upper side than on the lower side of VEP leaves even when predators were absent (and density of *B. obovatus* was moderate). The hatchability of *B. obovatus* eggs was nearly 90% on both sides of VEP leaves in the absence of predators. Therefore, oviposition by *B. obovatus* on the upper side of a VEP leaf (Chapter 2) could function as a means of predator avoidance.

On the other hand, although *B. obovatus* experiences lower levels of regulation by predatory mites on upper sides of leaves than on lower sides, their eggs may be exposed to greater environmental stresses on the upper leaf side; rainfall (Foott 1963), desiccation, radiant heat, and solar UVB radiation (Ohtsuka and Osakabe 2009; Onzo et al. 2010). The break-even point of declining predation risk and increasing environmental stresses on leaf upper sides will vary with spatiotemporal changes of stressors and the magnitude of environmental tolerance intrinsic to each mite species. The next chapter clarifies the effects of temperature (radiant heat) and solar UVB radiation on *B. obovatus* egg development and hatchability on the upper leaf surface of VEP.

Chapter 5
Solar radiation as a restring factor of the seasonal fluctuation in the availability of an upper leaf surface as an oviposition site of *Brevipalpus obovatus*

5-1 Introduction

The effects of temperature on mite communities have been examined extensively in literatures (Stenseth 1979; Roy et al. 2003; Stavrinides and Mills 2011) while the effects of solar ultraviolet (UV) radiation have been relatively less taken into consideration (Barcelo 1981). The deleterious effects of solar UVB (280–320 nm wavelengths) radiation on both herbivorous and predacious mites have been increasingly demonstrated in the recent literatures (Suzuki et al. 2009; Ohtsuka and Osakabe 2009; Onzo et al. 2010; Sakai et al. 2012b; Tachi and Osakabe 2012; Fukaya et al. 2013). UVB potentially constrains mites to lower leaf surface and inside domatia. However, the quality of upper (adaxial) leaf surface as food resource is not inferior to the lower (abaxial) surfaces for the herbivorous two-spotted spider mite *Tetranychus urticae* Koch (Acari: Tetranychidae) on kidney bean leaves (Sakai and Osakabe 2010) and the citrus red mite *Panonychus citri* (McGregor) on citrus leaves (Fukaya et al. 2013).

The level of UV damage is determined by the cumulative UVB irradiance in *T. urticae* (Murata and Osakabe 2013). This indicates that a change in the developmental rate (i.e., an increase or decrease in developmental duration) as a thermoresponse is related to the seasonally specific severity of UV damage (Sakai et al. 2012b; Murata and Osakabe 2013). Seasonal fluctuations in temperature and the intensity of solar UVB radiation are not precisely synchronized; Kyoto experiences relatively lower temperatures and higher UVB intensity in spring and higher temperatures and lower UVB intensity in autumn. Although the UVB dose-rate (daily cumulative irradiance) is highest in summer, the most serious UV damage to *T. urticae* eggs is caused in spring (Sakai et al. 2012b).

In Kyoto, west-central Japan, a false spider mite *Brevipalpus obovatus* occurs on VEP plants from late summer to mid-autumn (i.e., late August to October), during which they are coexisting with predacious phytoseiid mites, mainly *Phytoseius* spp. (Sudo et al. 2010). One-third of eggs and ~10% of motile individuals of *B. obovatus* remain on adaxial (upper) leaf surfaces of VEP (Chapter 2). In contrast, almost the entire phytoseiid mite population of *Phytoseius nipponicus*, a generalist

predator that prey on *B. obovatus* eggs, resides on the abaxial (lower) leaf surfaces throughout the seasons (Sudo et al. 2010; Chapter 2). Phytoseiid mites sensitively avoid solar radiation (Tachi and Osakabe 2012). Furthermore, an adult *P. nipponicus* shows a positive geotaxis, i.e., it prefers to stay the underside of a leaf (Chapter 4). As a result, *B. obovatus* eggs are less frequently preyed upon by *P. nipponicus* on the upper leaf surfaces than on the lower leaf surfaces, suggesting that ovipositing on upper leaf surface serve to avoid predation unless the eggs are eradicated by solar UVB or other environmental stresses such as heat stress.

Pant-dwelling mites are susceptible to heat stress between 30 and 35°C in Japan (Kiritani 2012, 2013). Monthly means of the daily average and highest temperatures over the last decade (2003–2012) were 27.0 ± 1.4 (SD) and 31.7 ± 1.9°C in July, respectively, and 28.5 ± 0.9 and 33.7 ± 1.1°C in August, respectively, in Kyoto (http://www.jma.go.jp/jma/indexe.html). Mites exposed to radiant heat on upper leaf surfaces, and thus the upper leaf surface user such as *B. obovatus* may suffer substantial heat stress in summer. Seasonal fluctuations of solar UVB intensity and temperature (including radiant heat) are likely to restrict the availability of upper leaf surfaces. Therefore, I hypothesized that the seasonal demography of *B. obovatus* is determined by the interaction between solar UVB irradiance and temperature.

In this chapter, seasonal changes in the effect of solar radiation on the fate of *B. obovatus* eggs were investigated in relation to the interaction between UVB irradiance and temperature effects (developmental rate and heat stress). First, I assessed the vulnerability to UVB radiation and thermoresponses of eggs in laboratory experiments. Second, the hatchability of eggs exposed to UV-manipulated solar radiation was investigated from spring (May) to autumn (October), and the effects of UVB and temperature were evaluated using statistical models. Finally, I established a best-fit deterministic model and predicted how solar UVB radiation and temperature affect seasonal fluctuations of egg survival on upper leaf surfaces.

5-2 Materials and methods

5-2-1 Mites

Brevipalpus obovatus was collected from VEP leaves in September 2009 in a secondary broadleaf forest in Iwakura. The mites were reared on VEP leaf disks placed abaxial-surface-up on water-soaked cotton in Petri dishes in the laboratory at 25°C with a 16:8-h light-dark photoperiod. VEP leaves were collected from Iwakura when necessary. Adult females that were five- to 15-days-old after the adult emergence were used for experiments. On the basis of their life history, female mites were expected to produce eggs throughout the experimental period (Goyal et al. 1985; Chapter 3).

5-2-2 Host plant leaves

The VEP leaves used for the experiments (test leaves) were collected from two potted shrubs in a greenhouse. The petiole of each leaf was coated with acrylic emulsion adhesive (#10824, Konishi, Osaka, Japan) to prevent the leaf surface from flooding with water. Then, the leaves were placed on water-soaked cotton in a Petri dish (9 cm in diameter). In all experiments, I took a photograph of each test leaf, and the oviposition sites of all *B. obovatus* eggs were individually mapped on the printed A4-size photograph to precisely determine the fate of each egg.

5-2-3 Laboratory experiments on the vulnerability of eggs to UVB radiation

Laboratory experiments were conducted at 25°C with a 16:8-h light-dark photoperiod. Ten adult *B. obovatus* females were introduced to each of the four VEP leaves (abaxial surface up) in a Petri dish and allowed to lay eggs for 24 h. The position of each newly oviposited *B. obovatus* egg was recorded every 24 h under a stereomicroscope (20×). Mite adults were removed from leaves 1 day after introduction.

Immediately after removal of mite adults, leaves were placed on a shelf (steel rack) at 25°C, and eggs were irradiated with a UVB lamp (YGRFX21711 GL, Panasonic Co., Osaka). The periphery of the shelf was covered with UV-opaque film (0.1-mm thick polyvinyl chloride film, Cutace Kirinain; MKV Platech Co. Ltd., Tokyo) that filtered out UV. Leaves were assigned to four treatments according to distance from the UVB lamp: UVB irradiation at (1) 0.58, (2) 0.31, and (3) 0.19 W m^{-2} for 1 h (cumulative irradiances of (1) 2.09, (2) 1.12, and (3) 0.68 kJ m^{-2}, respectively), and (4) no UVB irradiation (0 kJ m^{-2}: outside the shelf, as a control). UVB intensity at each irradiation site was measured using a UV meter ($X1_1$ Optometer, Gigahertz-Optik GmbH, Türkenfeld) equipped with a UVB detector head (UV-3702-4). Leaves of all treatments were also illuminated with 40-W fluorescent lamps affixed to a sidewall at 50-cm distance and 40-cm intervals. Figure 5-1 presents the spectra of relative ultraviolet/visible light intensity in situ; values were measured using a spectrometer (UFV-VIS F, Spectra Co-op Corporation, Tokyo).

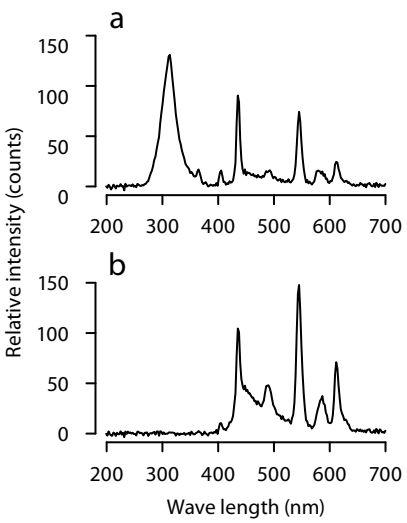

Fig. 5-1 Wavelength spectra measured on experimental shelves under artificial UVB irradiances at (a) 58 μW cm^{-2} and (b) 0 μW cm^{-2} (outside the shelf frame).

After irradiation, egg status was inspected daily, and the egg-hatching rate for each treatment was determined. Data collection was continued until the fates of all eggs were confirmed. The experiment was replicated five times (i.e., four cumulative UVB irradiances × five leaves). All replicates were conducted in June 2011. Different mite adults were used in each replicate.

The UVB dose–egg hatching success response was fitted to a generalized linear mixed model (GLMM: logit link, binomial errors), in which the explanatory variable is the cumulative UVB irradiance and the response variable was the proportion of eggs that successfully hatched on each leaf. Leaves in each replicate were clustered. The "glmmML" module (version 0.82-1: Broström and Holmberg 2011) of R version 2.15.1 (R Core Team 2012) was used.

5-2-4 Laboratory experiments on thermoresponses of eggs

The duration of the egg stage for *B. obovatus* population was tested under seven isothermal conditions: 15.2 ± 0.5, 18.8 ± 0.5, 22.8 ± 0.3, 29.0 ± 0.5, 32.6 ± 0.6, 34.2 ± 0.7, or 35.7 ± 0.7°C in incubators (Bio Multi Incubator LH-30-8CT, NK system, Osaka) at a 14:10-h light-dark photoperiod. These temperatures covered the thermal range of 20–30°C that is suitable for *B. obovatus* egg development (Goyal et al. 1985). For each temperature treatment, two (18.8, 22.8, 29.0, and 35.7°C), three (32.6 and 34.2°C), or four (15.2°C) VEP leaves were placed adaxial-surface-up on water-soaked cotton in 9-cm diameter Petri dishes. I used more leaves at the lower temperature in order to obtain the number of eggs equivalent to that at the higher temperature.

Ten *B. obovatus* adult females were introduced to each VEP leaf assigned to each thermal treatment. A data logger (17 mm in diameter, 6 mm in height; Hygrochron, KN Laboratories, Osaka) was placed on a piece of Parafilm (2.5 × 2.5 cm; PM-996, Pechiney Plastic Packaging Inc., Chicago) on water-soaked cotton in a Petri dish to collect temperature and relative humidity (RH) values every 30 min. The leaves and data logger were placed in a transparent plastic box (29.5 cm length × 22 cm width × 5 cm depth; up to two leaves and one logger in each box). The lid of the plastic box had an air vent (18 cm in diameter) covered with polyester mesh (Honey queen #9000, Toray Industries, Inc., Tokyo). To maintain RH on the disks at approximately 60%, 50–75% of the vent area was covered with polyvinyl chloride film (Riken Wrap, Riken Technos Co., Tokyo). The plastic box was placed in an incubator set at the assigned temperature.

Adult females were allowed to oviposit freely for 8 and 4 days at 15.2 and 18.8°C, respectively, and for 2 days at the other temperatures. The periods for oviposition were increased in treatments at the lower temperatures in order to obtain the similar amount of eggs as well as the number of leaves described above. The positions of newly oviposited eggs were mapped on the printed leaf photographs at 24 h intervals, and then, the females were removed. The status of each egg was inspected every 24 h until all eggs had hatched or died. If the hatching of a larva was interrupted for more than 24 h, the egg was recorded as "dead." The experiments were performed from May to June 2012.

The egg developmental rate (V) was defined as the reciprocal of the mean incubation period of hatched eggs in each temperature treatment. At a certain thermal range, the developmental rate (V) for a given temperature (t) can be represented as the following linear model (cf. Kiritani 2012):

$$V = A + Bt \quad (1),$$

where A and B are constants. Developmental zero (T_0) was defined as the x-intercept of the model

$$T_0 = -\frac{A}{B} \quad (2),$$

and the thermal constant (K) was obtained from

$$K = -\frac{1}{B} \quad (3).$$

The temperature–egg developmental rate relationship was fitted to a Gaussian GLMM, in which the explanatory variable is the temperature and the response variable was the developmental rate of each egg. Leaves were assigned to random factor. The "lmer" module of "lme4" library (version 0.999999-2: Bates et al. 2013) running on R version 3.0.1 (R Core Team 2013) was used.

5-2-5 Manipulative field experiments on the effects of solar radiation on egg survival

Brevipalpus obovatus eggs were exposed to sunlight under near-ambient (UV+) and UV-attenuated (UV–) conditions every month from May to October 2012. During each month, 12 VEP leaves (eight in the May experiment) were prepared (adaxial surface up) and randomly divided into 2 × 6 (or 2 × 4 in May) groups, representing two treatments for solar UV (UV+/UV–) and six (four) consecutive oviposition dates.

Thirty *B. obovatus* adult females were introduced to each of the two VEP leaves, one for UV+ and the other for UV–, in the laboratory in the morning (7:30 am; day 0) and allowed to lay eggs for 24 h. On the morning of the next day (day 1), the females were moved to the next two leaves at random (but in even numbers) using a fine paintbrush. This procedure was repeated over 6 days (or 4 days in May). Consequently, I obtained the six (or four) groups of eggs within 24 h after oviposition.

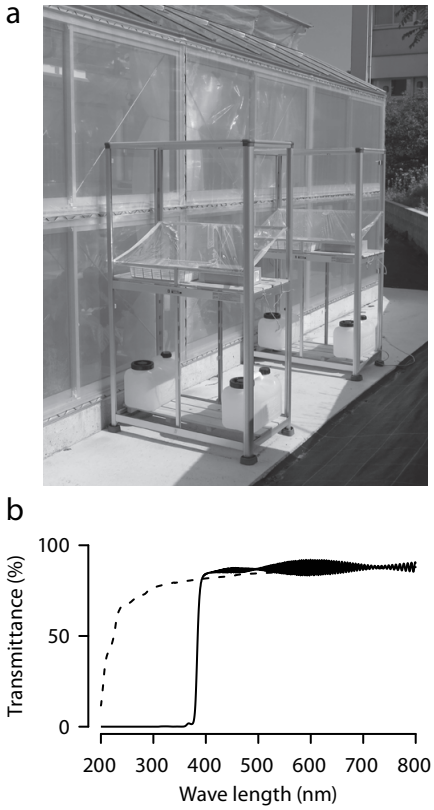

Fig. 5-2 Experimental set-up to test the solar UVB effect on *Brevipalpus obovatus* eggs. (a) Experimental shelves used to attenuate solar UVR (front: the UV– apparatus, back: the UV+ apparatus). The roof of each shelf was south-facing and pitched to allow rainwater to run off. (b) Transmission spectra of light under UV-transparent polyethylene film (solid line) or UV-opaque polyester film (dashed line) used for the roofs of the UV+ or UV– shelves, respectively.

On the morning (8:00 am) of day 1, one leaf assigned to UV+ was set on a shelf covered with UV transparent film (polyethylene film, 30-μm thick; Dainichi Sangyo Co. Ltd., Osaka), and the other leaf, assigned to UV−, was set on a shelf covered with UV opaque film (HB3 polyester film, 25-μm thick; Teijin DuPont Films, Tokyo). Both shelves were placed in a test field at Kyoto University (35°1'52.5"N, 135°47'10.3"E, 70 m a.s.l.; Fig. 5-2a). The UV opaque film filtered out more than 90% of UV at wavelengths less than 380 nm (UVC, UVB, and most UVA) and more than 99% at wavelengths less than 363 nm (Fig. 5-2b). The UV transparent film allowed 72.5% transmittance at 280 nm. Both films transmitted 87% of wavelengths between 388 and 800 nm (visible light and a portion of UVA).

The leaves on the shelves were exposed to sunlight through UV transparent or opaque film in the morning (from daybreak to 13:00). Subsequently, sunlight reached the shelves through the wall of a greenhouse adjoining the shelves in the afternoon (from 13:00 to sunset) (Fig. 5-2a). Because wild VEP plants generally grow at forest edges and in canopy gaps, mites on VEP leaves may be exposed to sunlight for several hours a day, but not over the entire daytime. On the basis of monitoring using the UV meter on a sunny day during each experimental period, UVB transmittance to UV+ treatments was estimated at 70–75% and 40% of the intensity of direct solar radiation for the morning and afternoon, respectively. In contrast, UVB transmittance to UV− was 0.9–1.0% and 0.4–0.7% in the morning and afternoon, respectively. Temperature and RH values on the shelves were logged every 30 min throughout the experimental periods using the data loggers.

Eggs were reared on the shelves until all the eggs had hatched or died, unless a storm struck the experimental site (leaf disks were kept temporarily in the adjoining greenhouse for the following storm periods: 15 May, 8–9 June, 17 June, 19–22 June, and 10 November, during which the UVB irradiance was considered zero). Therefore, the eggs experienced temperature conditions at near those of the field environment.

After sunset every day during the experimental periods, VEP leaves were temporarily (within 45 min) brought to the laboratory, and the status of eggs was inspected. If the hatching of a larva was interrupted for more than 24 h, the egg was recorded as "dead." I also judged eggs as dead when the contents were bleached or dried up. For each month, the proportion of eggs that successfully hatched in UV+ and UV− treatments were compared using 2 × 2 Fisher's exact tests. The "fisher.test" module of R 2.15.1 was used.

Evaluation of the effects of months and UV attenuation on the egg incubation period

To investigate the possibility of solar UV radiation causing an elongation of egg incubation periods in *B. obovatus*, GLMMs (log-link, Poisson errors) were constructed, in which the explanatory variables were month (May to October as a categorical variable), UV treatment (UV+ or UV−), and their two-way interaction. The response variable was the incubation period of each hatched egg. Leaf disks on which each egg was laid were assigned random-effect status in mixed modeling

to prevent pseudo-replication. The combination of possible models containing all or some of the explanatory variable(s) was examined, and the suitable version was selected using AIC. The "glmmML" module (version 0.82-1: Broström and Holmberg 2011) of R 2.15.1 was used.

Evaluation of the effect of cumulative UVB irradiance on egg hatching success in each month

The level of solar UVB irradiation during the experimental period was estimated based on data released by the Solar Radiation and Weather Monitoring Project at Kyoto Women's University (34°59'19"N, 135°46'49"E; http://www.cs.kyoto-wu.ac.jp/~konami/climate/index.shtml), 4.8 km south of the experimental site. Global UVB intensity (unit: W m^{-2}) was measured every 5 s (data for August 19–20 were missing).

The cumulative UVB irradiance for the whole incubation period were calculated for each hatched egg as the products of the solar UVB intensities and the UVB transmittances to the shelves, which were determined as 70% and 40% for the UV+ shelf in morning (from 0:00 to 13:00) and afternoon (from 13:00 to 24:00), respectively, and 1.0% and 0.7% for UV– in the morning and the afternoon, respectively.

Deleterious effect of solar UV radiation on *B. obovatus* eggs was evaluated by the following manner. For the UV+ treatment, the mean cumulative UVB irradiance during the egg incubation period was calculated for each oviposition date-group of eggs (32 groups in total: including both hatched and dead eggs), except for the groups on 19 and 20 August (missing UVB data). Then, these data were fitted to a one-way GLMM (logit-link, binomial errors) and evaluated using a Wald test. The explanatory and response variables were the mean of cumulative UVB irradiance and the egg hatchability (the proportion of egg hatched successfully) for each oviposition date-group, respectively. The coefficient of determination (McFadden's pseudo R^2; McFadden 1974) was also calculated for the fitted GLMM. The mean daily UVB irradiances were also calculated for the egg groups in the UV+ treatment and fitted to a binomial GLMM. The explanatory and response variables were the mean daily UVB irradiance and the egg hatchability for each oviposition date-group, respectively. The R module "glmmML (version 0.82-1)" was used to fit the GLMMs.

Evaluation of the effects of high temperature (heat stress) on egg hatching success

In terms of high temperature damage, on the basis of the temperature datasets logged on the shelves, the mean daily maximum temperature during the incubation period for each egg was calculated and averaged for each oviposition date and UV treatment. The resulting datasets for UV+ and UV– treatments were then separately fitted to the one-way GLMM (logit-link, binomial errors) and evaluated using a Wald test. The explanatory and response variables were the mean daily maximum temperature and the egg hatchability for each oviposition date, respectively. The coefficients of determination for the fitted models were also calculated for the fitted GLMMs. I also evaluated the effects of high temperatures on egg hatchability using datasets from the Kyoto Local

Meteorological Observatory (35°00'54"N, 135°43'53"E), Japan Meteorological Agency (http://www.data.jma.go.jp/obd/stats/etrn/index.php).

Evaluation of the interactive effects of UVB irradiance and high temperature

Two-way GLMMs (logit-link, binomial errors) were used to evaluate the interactions between UVB irradiance (the cumulative irradiance or the mean daily irradiance during incubation periods) and high temperature dose and how they affect the hatchability of *B. obovatus* eggs. The model contained the (cumulative or mean daily) UVB irradiance value, the mean daily maximum temperature during the incubation period, and their interaction as explanatory variables, and the egg hatchability for each oviposition date-group as a response variable. The mean daily maximum temperatures were calculated on the basis of the datasets from the Kyoto Local Meteorological Observatory. The data from UV+ and UV− treatments were fitted to a single model.

5-2-6 Modeling egg survivability based on the seasonal dynamics of temperature and solar UVB intensity

On the basis of the egg-development parameters obtained from the above-mentioned experiments, an individual-based deterministic model was constructed to assess how the deleterious effects of solar UVB radiation and high temperature seasonally affect the egg survivability of *B. obovatus* on the upper surface of a plant leaf. First, the egg incubation period was estimated for each of the oviposition dates from 1 March 2002 to 15 October 2012 using the solar UVB dataset from Kyoto Women's University and the air temperature dataset provided by Kyoto Local Meteorological Observatory. The effective temperature was calculated for every 1 h during the 11 years. The dataset contained two missing data points: 1:00 am on 15 March 2005 and 1:00 am on 5 October 2010; each of these points was substituted with the mean of the temperature values measured in the preceding and following hour.

The relationship between temperature and the egg developmental rate was represented by a model consisting of three parameters: the lower threshold (K_1: same as the developmental zero T_0), upper threshold (K_2: egg developmental rate would increase from K_1 to K_2), and upper limit (K_3). An egg would develop at a constant rate between K_2 and K_3, and an egg would not develop above K_3 (Baskerville and Emin 1969). The above-mentioned isothermal experiment was used to determine these parameters: K_1 = 12.7°C, K_2 = 29.0°C, and K_3 = 35.0°C. The thermal constant (K) of *B. obovatus* was also determined as 98.8 day-degrees [formula (3)]. Each egg was assumed to have been laid on a host leaf at 5:00 am of the first day and hatch after sunset of the day on which the cumulative effective temperature reached the thermal constant.

The temperature on an upper leaf surface was expected to be higher than the air temperature owing to the radiant heat of sunlight, and solar UVB exposure delayed the egg incubation period (Table 2). Therefore, prior to the estimation of egg hatchability, the incubation period predicted

from air temperature data and the thermoresponse model was compensated to fit the actual incubation period under sunlight. The results of the UV+ treatment were fitted to a one-way linear model. The explanatory and response variables were the predicted egg incubation periods and the actual incubation periods of the hatched eggs for the corresponding oviposition dates, respectively. Then, the relationship was used for the compensation of the predicted egg incubation periods. The "lm" and "predict" functions in R 2.15.1 were used for the linear regression and calculation of the 95% prediction interval, respectively.

For each oviposition date between 1 March 2002 and 15 October 2012, the cumulative UVB irradiance and the mean daily maximum temperature were estimated based on the predicted (and compensated) incubation period of a *B. obovatus* egg. The level of solar UVB irradiation during this period was estimated based on the dataset from Kyoto Women's University. To estimate UVB-induced damage at the same irradiation level within the UV+ treatment of the outdoor experiment in 2012, UVB irradiation was determined as 70% or 40% of the value from unobstructed sky in the morning (from 0:00 to 13:00) or afternoon (from 13:00 to 24:00) of each day, respectively. The air temperature dataset from the Kyoto Local Meteorological Observatory was used for the calculation of mean daily maximum temperatures.

5-3 Results

5-3-1 Laboratory experiments on the vulnerability of eggs to UVB radiation

UVB dose–egg hatching success response of *B. obovatus* was obtained from 188 eggs. The egg hatching success decreased with increased cumulative UVB irradiance, whereas most eggs hatched successfully in controls without UVB irradiation (Fig. 5-3). LD_{50} value of UVB for mite eggs was calculated 2.35 kJ m^{-2}.

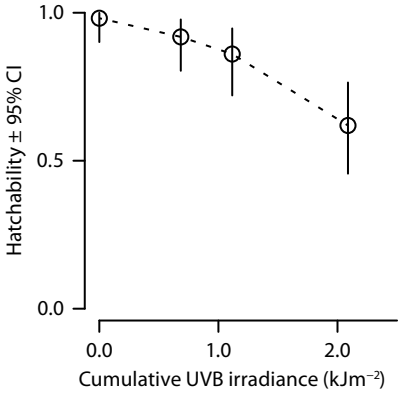

Fig. 5-3 Dose response for the lethal effects of artificial UVB irradiation on *Brevipalpus obovatus* eggs.

5-3-2 Thermoresponses of eggs

More than 80% of *B. obovatus* eggs hatched within a temperature range of 15.2–34.2°C (Table 5-1). In contrast, no eggs hatched at 35.7°C, indicating high temperature damage. The developmental rate of eggs at each temperature increased linearly from 15.2°C to 29.0°C (Fig. 5-4). In contrast, developmental rates at 32.6°C and 34.2°C remained at the same level as those observed for 29.0°C. Developmental zero (T_0) and the thermal constant (K) were calculated as 12.7°C and 98.8 day-degrees, respectively.

Table 5-1 Egg hatchability and incubation periods at seven constant temperature conditions

Temperature (˚C) (mean ± SD)	No. of eggs	% hatchability	Incubation period (days) (mean ± SD)
15.2 ± 0.5	87	82.8	36.9 ± 2.2
18.8 ± 0.5	80	97.5	16.8 ± 0.8
22.8 ± 0.3	67	100	10.2 ± 0.7
29.0 ± 0.5	106	100	5.99 ± 0.4
32.6 ± 0.6	158	89.9	6.17 ± 0.7
34.2 ± 0.7	128	83.6	6.22 ± 0.6
35.7 ± 0.7	82	0.0	—

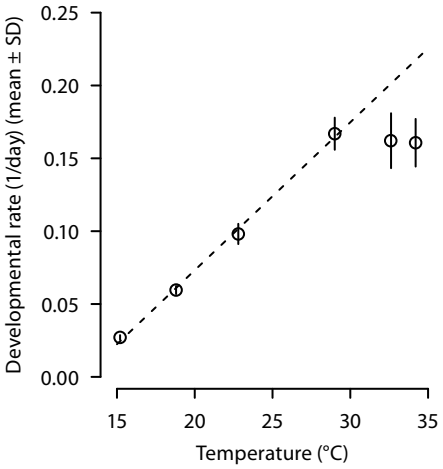

Fig. 5-4 Developmental rate (open circles) of *Brevipalpus obovatus* eggs at different temperatures. Data at 35.7°C were not shown because no eggs hatched. The relationship between temperature (*t*) and developmental rate (*V*) was fitted to the following linear model: $V = -0.1285 + 0.01012t$.

5-3-3 Effects of solar radiation on egg survival

Egg hatchability was lowest in July and highest in October in both the UV+ (1.84% and 66.0%, respectively) and UV− (0.50% and 94.6%, respectively) treatments (Fig. 5-5a). Attenuation of solar UV significantly increased egg hatchability in May, June, September, and October (2×2 Fisher's exact tests, $P < 0.01$) and marginally so in August ($P = 0.06657$), whereas most eggs died regardless of UV manipulation in July.

Mean temperatures on the experimental shelves over the monthly experimental periods did not significantly differ between the UV+ (14.3–31.2˚C) and UV− treatments (14.2–31.2˚C; Table 5-2; Welch two-sample *t*-test, $t = -1.4592$, $df = 14098.09$, $P = 0.1445$). Mean RH was slightly higher in UV+ [70.8% (59.7–78.5%)] than in UV− treatments [69.4% (59.2–76.2%); Welch two-sample *t*-test, $t = 4.3286$, $df = 14064.72$, $P < 0.001$], but this difference was unlikely to affect egg hatchability.

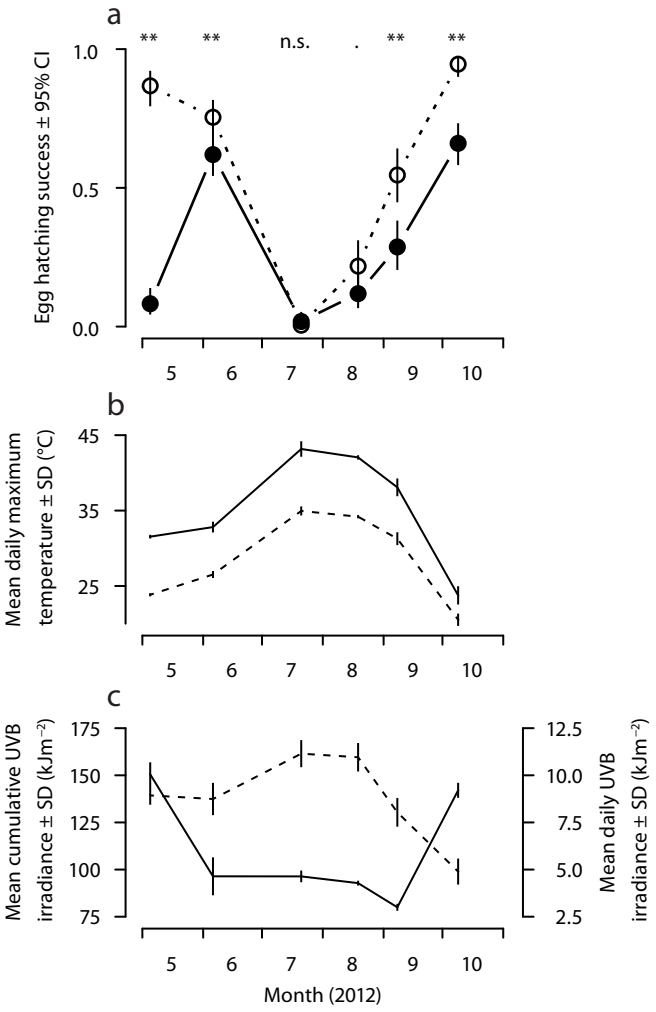

Fig. 5-5 (a) Seasonal changes (May to October 2012) of *Brevipalpus obovatus* egg hatching success under near-natural conditions (UV+: filled circles connected by solid lines) and UV-attenuated conditions (UV–: open circles, dashed line). Asterisks at the top of plots indicate significant differences between hatching success in the UV+ and UV– treatments at levels of 0.1 (.) or 0.01 (**) (2 × 2 Fisher's exact tests). Vertical bars represent 95% CIs.
(b) Seasonal fluctuation of mean daily maximum temperature measured in the UV+ experimental apparatus (solid line) and the Kyoto Local Meteorological Observatory (broken line).
(c) Seasonal fluctuation of mean cumulative UVB irradiance (solid line) and mean daily UVB irradiance (broken line) in the UV+ conditions. Mean temperature and the mean UVB irradiances were calculated based on the actual incubation period of every egg that hatched successfully in each month and UV condition.

Evaluation of the effects of months and UV attenuation on the egg incubation period

Egg incubation period in UV+ elongated roughly to 110% of that in UV– in all months except July (only four eggs hatched in July) (Table 5-2). The GLMM data fitting and subsequent model selection substantiated the significance of the effects of month and UV attenuation on egg incubation period, but their two-way interaction was not significant (AIC = 164.1 versus 173.7 for the models without or with the interaction, respectively). Solar UVB radiation may cause an elongation of the duration of the egg stage (e.g. Adams and Shick 2001). Consequently, the cumulative UVB irradiance for the incubation period of eggs in UV+ was highest in May (150.5 kJ m^{-2}) and lowest in September (79.9 kJ m^{-2}), whereas values were consistently low in UV– (1.13–2.18 kJ m^{-2}; Table 5-2).

Evaluation of the effect of the cumulative UVB dose and the daily UVB dose on egg hatching success

The cumulative UVB irradiance, which is a function of both UVB intensity and the duration of the egg stage, is a determinant of the hatchability of *T. urticae* eggs (Sakai et al. 2012b; Murata and Osakabe 2013). However, the effect of cumulative UVB irradiance on egg hatchability in UV+ was not significant in the one-way binomial GLMM and subsequent Wald test (df = 1, z = –1.0170, P =

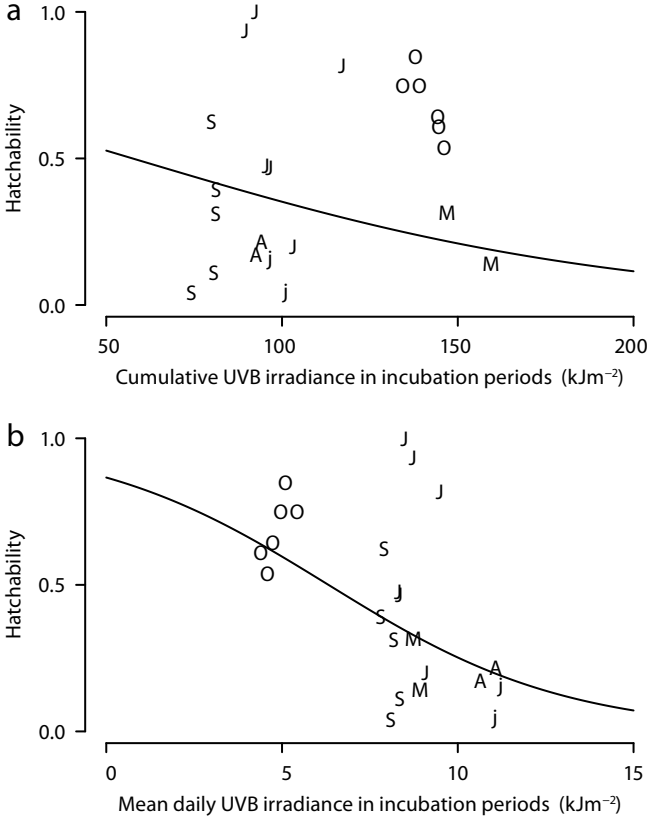

Fig. 5-6 The effect of solar UVB exposure on egg survival of *Brevipalpus obovatus*, showing the relationship between egg hatchability in the UV+ treatment and (a) cumulative UVB irradiance during the incubation periods and (b) the mean daily UVB irradiance. Each plot represents the cohort (i.e. the groups of eggs laid on each day of the month) for each month: May (M), June (J), July (j), August (A), September (S), or October (O) of 2012.
The relationship between the cumulative UVB irradiance (x) and egg hatchability (p) was fitted to the following binomial logit model (curve in plot): $p = 1 / [1 + \exp(-0.82307 + 0.01432x)]$. The relationship between the daily UVB irradiance (x) and egg hatchability (p) was fitted as $p = 1 / [1 + \exp(-1.8679 + 0.2955x)]$.

0.309; Fig. 5-6a). The egg hatchability of *B. obovatus* was very minimally explained by the cumulative UVB irradiance alone during the egg period (McFadden's pseudo $R^2 = 0.0097$). In contrast, egg hatchability in UV+ was negatively correlated with the mean daily UVB irradiance during the incubation period (Wald test, $df = 1$, $z = -2.251$, $P = 0.0244$; McFadden's pseudo $R^2 = 0.0231$; Fig. 5-6b), potentially contradicting the reciprocity law (Murata and Osakabe 2013).

Evaluation of the effects of high temperature (heat stress) on egg hatching success

In terms of high temperature damage, the mean daily maximum temperatures measured on the experimental shelves during the incubation periods within date-groups significantly negatively affected egg hatchability in both UV+ (Wald test, $df = 1$, $z = -2.02$, $P = 0.0434$) and UV– treatments ($df = 1$, $z = -9.942$, $P = < 2.00 \times 10^{-16}$). The deleterious effect of high temperature explained the decline in egg hatchability to some extent in UV– (McFadden's pseudo $R^2 = 0.115$) but did not in UV+ (McFadden's pseudo $R^2 = 0.0141$). Better fitting to the egg hatchability data was obtained from statistical analyses using the temperature dataset provided by the Kyoto Local Meteorological Observatory in both UV+ (Wald test, $df = 1$, $z = -2.798$, $P = 0.00515$; McFadden's pseudo $R^2 = 0.0395$; Fig. 5-7a) and UV– (Wald test was not conducted; McFadden's pseudo $R^2 = 0.272$; Fig. 5-7b). For the following analyses of interactive effects, I used the datasets from the Kyoto Local Meteorological Observatory.

Table 5-2 The effect of UV attenuation on egg hatchability and incubation period of *Brevipalpus obovatus* in each season

Start date[*1] (2012)	Treatment (no. eggs tested)	Incubation period[*2] (days; mean ± SD)	Temperature (°C; upper) and RH (%; lower) (mean ± SD)	Mean cumulative UVB irradiance[*3] (kJ m^{-2})
05–08 May	UV+ (181)	16.88 ± 0.99 (1.08)	20.8 ± 7.0 59.7 ± 20.9	150.5
	UV– (182)	15.58 ± 1.19	20.8 ± 6.9 59.2 ± 19.9	2.18
06–11 Jun	UV+ (171)	11.08 ± 1.18 (1.10)	24.3 ± 5.4 71.8 ± 18.4	96.4
	UV– (171)	10.09 ± 0.84	24.2 ± 5.2 70.5 ± 17.1	1.34
21–26 Jul	UV+ (163)	8.33 ± 0.58 (0.926)	31.2 ± 6.5 66.3 ± 18.6	96.4
	UV– (199)	9.00	31.2 ± 6.6 65.6 ± 17.6	1.57
19–24 Aug	UV+ (118)	8.78 ± 0.70 (1.10)	30.8 ± 6.0 65.1 ± 17.2	92.8
	UV– (101)	7.95 ± 1.09	30.6 ± 5.8 65.1 ± 16.1	1.24
08–13 Sep	UV+ (108)	10.03 ± 0.95 (1.13)	26.8 ± 6.1 72.0 ± 18.3	79.9
	UV– (108)	8.88 ± 0.93	26.4 ± 5.6 71.5 ± 16.6	1.13
09–14 Oct	UV+ (162)	29.58 ± 4.38 (1.11)	14.3 ± 5.3 78.5 ± 14.7	142.0
	UV– (157)	26.71 ± 2.71	14.2 ± 5.1 76.2 ± 13.9	1.98

[*1] It signifies the series of days in which the exposure for each egg started.

[*2] Figures in parentheses represent the ratio of incubation periods in UV+ to UV–.

[*3] Cumulative irradiances were calculated for the actual incubation period of every egg that hatched successfully.

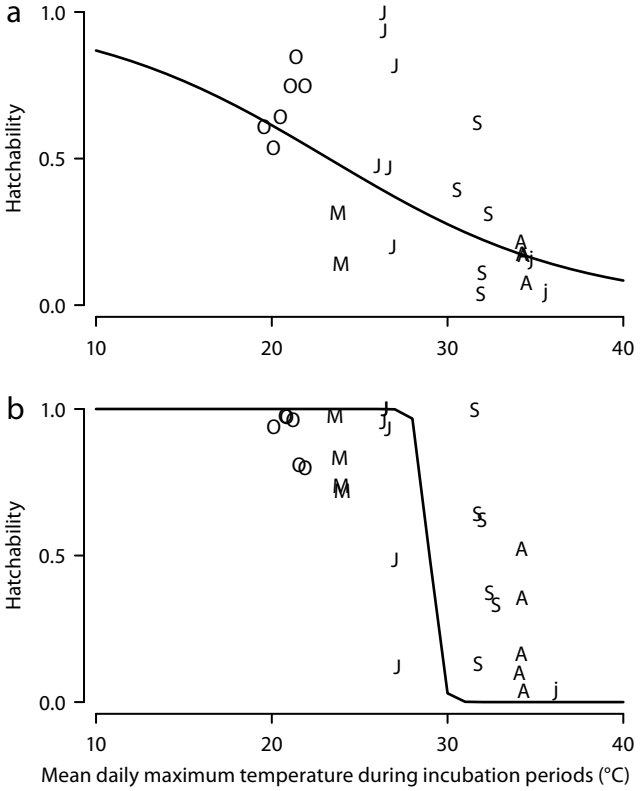

Fig. 5-7 The effect of high temperature on egg survival in *Brevipalpus obovatus*, showing the relationship between egg hatchability in (a) UV+ or (b) UV– treatments and mean daily maximum temperature measured in the Kyoto Local Meteorological Observatory during the egg incubation periods. Each plot represents the cohort (the groups of eggs laid on each day of the month). The relationship between the mean maximum temperature (x) and egg hatchability (*p*) was fitted to the following binomial logit models: $p = 1 / [1 + \exp(-3.3166 + 0.1427x)]$ in UV+; $p = 1 / [1 + \exp(-99.364 + 3.428x)]$ in UV–.

Evaluation of the interactive effects of UVB irradiance and high temperature

The interactive effect between the cumulative UVB irradiance and mean daily maximum temperature from the datasets provided by the Kyoto Local Meteorological Observatory during the incubation period on egg hatchability was supported by the following two-way binomial GLMM and subsequent model selection (i.e., the model containing the two-way interaction was selected; AIC = 314.6 versus 327.2; Fig. 5-8):

$$p = -\frac{1}{1 + e^{(-10.45623+0.04265x+0.34872y-0.00114xy)}} \qquad (4),$$

where 'x' is the cumulative UVB irradiance (kJ m^{-2}), 'y' is the mean daily maximum temperature (°C), and 'p' is the egg hatchability for each oviposition date-group.

This saturated model provided a better fit to egg hatchability in (McFadden's pseudo $R^2 = 0.356$) than the above-mentioned one-way models containing the cumulative UVB irradiance, the mean daily UVB irradiance, or the mean daily maximum temperature. Although the interactive effect between mean daily UVB irradiance and mean daily maximum temperature on egg hatchability was also supported by a two-way binomial GLMM (AIC = 342.4 and 377.0 for models with and without the two-way interaction, respectively), the models provided a weaker fit to egg hatchability in (McFadden's pseudo $R^2 = 0.298$). Therefore, the strong correlation between the mean daily UVB irradiance and egg hatchability obtained from the one-way binomial GLMM analysis was likely a spurious correlation because of the omission of a high-temperature effect.

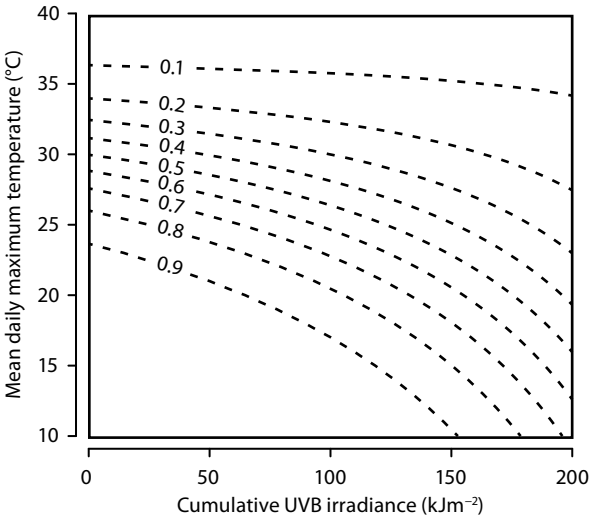

Fig. 5-8 Estimation of *Brevipalpus obovatus* egg hatchability based on the doses of solar UVB and temperature. The effects of cumulative UVB irradiance (x: as kJm^{-2}) and mean daily maximum temperature (y) during the egg incubation period on the hatchability (p) were fitted to the two-way GLMM (logit-link, binomial errors). The contours (broken lines) represent the estimated egg hatchability at given condition of UVB (x-axis) and temperature (y-axis). The mean daily maximum temperatures were calculated based on the air temperature data measured at the Kyoto Local Meteorological Observatory.

5-3-4 Modeling egg survivability based on seasonal dynamics of temperature and solar UVB intensity

On the basis of the long-term temperature dataset from Kyoto, the egg incubation period of *B. obovatus* was predicted for each of the oviposition dates from 1 March 2002 to 15 October 2012 (3882 days). The results of the UV+ treatment in the outdoor experiment in May to October 2012 were fitted to the following linear model (Fig. 5-9):

$$y = -0.231149 + 1.23529x \qquad (5),$$

where x and y are the predicted egg incubation period (days) for each oviposition date in the experiment and the actual mean incubation period (days) of the hatched eggs laid on the corresponding oviposition dates in the UV+ treatment, respectively. The predicted egg incubation period was calculated based on the temperature measured every 1 h at the Kyoto Local Meteorological Observatory. This regression provided a strong correlation (adjusted $R^2 = 0.92$); thus, formula (5) was used for the compensation of the egg incubation period. The predicted (and compensated) egg incubation periods of *B. obovatus* decreased with time from January to June in each year. Subsequently, the incubation period remained at around 9–10 days during summer (July, August, and early September) but rapidly increased in autumn as temperatures declined. If an egg was laid on a leaf in November or December, it was predicted to hatch the following spring.

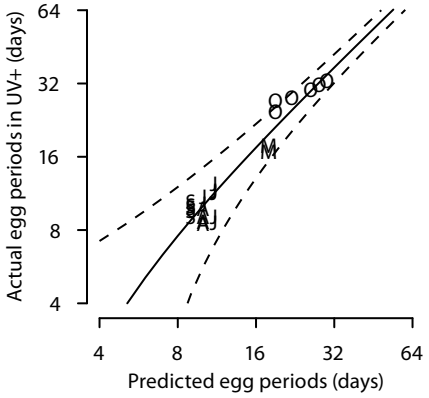

Fig. 5-9 The relationship between the predicted and actual egg incubation period of *Brevipalpus obovatus*. Each plot represents the cohort (the groups of eggs laid on each day of the month). The results of linear regression (solid line) and its 95% prediction intervals (dashed lines) are also shown; the relationship between predicted (x) and actual (y) incubation periods was fitted as $y = -0.29258 + 1.05541x$.

The complete dataset of cumulative UVB irradiance and mean daily maximum temperature during the estimated incubation periods was available for 1600 of the 3882 days (1 March 2002–15 October 2012). The estimated UVB irradiance reached minimal values twice a year, in late June [109 ± 21.4 kJ m^{-2} (mean ± SD)] and early August (98.4 ± 13.0 kJ m^{-2}; Fig. 5-10a). The mean daily maximum temperature during the predicted egg incubation periods was estimated to be highest for eggs oviposited in early August (34.0 ± 1.48°C) (Fig. 5-10a). Values then decreased rapidly in autumn and reached the minimum for the year in eggs oviposited in early December (14.9 ± 0.429°C).

Doses of UVB radiation and heat for the estimated egg incubation periods were applied to formula (4) to simulate the seasonal dynamics of egg hatching success of *B. obovatus*. The hatchability of eggs that were oviposited on each of the 1600 days was calculated and then stratified according to season (early or late half of each month; n = 6–133 days for each half-month). The predicted hatchability exhibited two clear peaks, one from May to June and the other from late September to October (Fig. 5-10b). Egg hatchability was higher at the latter peak in autumn [early October: 0.550 ± 0.0728 (mean ± SD)] than at the peak from late spring to early summer [highest in late May: 0.345 ± 0.0806 (mean ± SD)].

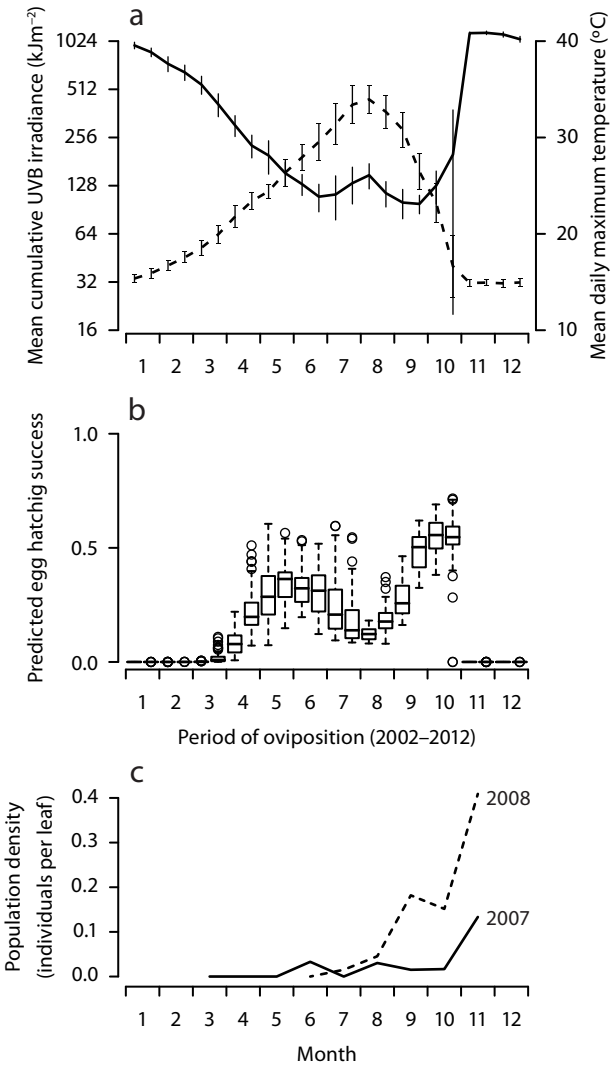

Fig. 5-10 (a) Seasonal fluctuations in the mean cumulative UVB irradiance (solid line) and mean daily maximum temperature (dashed line) for the predicted egg incubation periods of *Brevipalpus obovatus* in Kyoto. Each of the error bars shows the mean ± SD of the prediction for the oviposition dates from 2002 to 2012, pooled for every half-month.
(b) Seasonal fluctuation in the estimated egg hatching success. Open circles signify the outliners beyond the 1.5 times the interquartile range (whiskers in each box).
(c) Seasonal occurrence of *B. obovatus* on wild VEP plants in Iwakura, Kyoto (based on Sudo et al. 2010), showing the density of motile individuals per leaf collected once a month within the period from March to November of 2007 (solid line) and from June to November of 2008 (dashed line).

5-4 Discussion

The UV-manipulated field experiments revealed that solar UVB radiation is an essential determinant of the seasonal demography of *B. obovatus* populations experiencing heat stress. In *T. urticae*, which usually resides on lower leaf surfaces, linear relationships (using one-way analyses) between the cumulative UVB irradiance and the egg hatchability have been found in not only laboratory experiments using a UVB lamp (Murata and Osakabe 2013), but also in field UV-manipulation experiments (Sakai et al. 2012b). However, in *B. obovatus*, a one-way analysis revealed that the cumulative UVB irradiance scarcely explained the seasonal fluctuation of the hatching success of eggs exposed to solar UVB radiation. Instead, the two-way model including cumulative UVB irradiance and mean daily maximum temperature provided a better fit for explaining seasonal fluctuations of egg survival.

The LD_{50} values of *B. obovatus* eggs under UVB radiation from a UVB lamp (2.4 kJ m^{-2}) were four times higher than the LD_{50} values of *T. urticae* eggs (lower leaf surface user) in the study of Murata and Osakabe (2013) (0.58 kJ m^{-2}). However, the LD_{50} value for *B. obovatus* is too low to compare with the cumulative UVB irradiance in the UV-manipulated field experiments. Such differences between damage caused by the UVB lamp and solar UVB radiation have been noted for *T. urticae* eggs (Murata and Osakabe 2013). The LD_{50} value caused by solar UVB radiation was about 50 kJ m^{-2} (Sakai et al. 2012b), which was 86 times the LD_{50} value caused by the UVB lamp (Murata and Osakabe 2013). Santos (2005) reported recovery from UVB damage via photoreactivation caused by visible light in *T. urticae* and a mold mite *Tyrophagus putrescentiae* (Schrank). One potential mechanism causing such variation may be the photoenzymatic repair of UVB-induced DNA damage, which is driven by energy of UVA and visible light (Kalthoff 1975; Sinha and Häder 2002; Macfadyen et al. 2004).

These results imply that *B. obovatus* eggs are better protected from UVB compared to *T. urticae* eggs and may thus be tolerant to higher intensities of solar UVB radiation, e.g., >100 kJ m^{-2}. Nevertheless, the incubation period of a *B. obovatus* egg is around 8 or 9 days even in the summer. Even at the same UVB intensity, the severity of UV damage would be affected by temperature. Lower temperatures elongate mite development, resulting in a higher cumulative irradiance of UVB radiation that potentially reaches >200 kJ m^{-2} in spring and >100 kJ m^{-2} in summer, in turn retarding the survival of eggs. Furthermore, the results of field experiment show that exposure to solar UVB radiation lengthened the duration of egg stage.

Mite eggs laid on upper leaf surfaces are also exposed to heat stress by solar radiation. *Brevipalpus obovatus* retained higher resistance to high temperature compared to other herbivorous mites such as Tetranychidae. Although no eggs hatched at 35.7°C, hatchability was 83.6% at 34.2°C. This value may represent one of the highest upper developmental thresholds in herbivorous mites

(Kiritani 2012; Ullah et al. 2012). Nevertheless, the means and standard deviations of temperatures indicated that temperatures on the experimental shelves frequently exceeded 35°C in July and August. Meteorological datasets provided by the Japan Meteorological Agency (http://www.data.jma.go.jp/obd/stats/etrn/index.php) also indicated that the maximum air temperature in Kyoto (the experimental site) exceeded 35°C for 9 and 11 days in July and August 2012, respectively. Consequently, the seasonal fluctuations of egg hatchability in *B. obovatus* were not explained by a one-factor model but were instead better represented by a two-way model including the cumulative UVB irradiance and mean daily maximum temperature.

Considering the deleterious effects of solar UV and high temperature (radiant heat), the availability of upper leaf surfaces as an oviposition site for mites was predicted to be highest in autumn (September and October) rather than in early summer (May and June). While the average daily temperature during the incubation period did not significantly differ between the two seasons (cf. Fig. 5-5b), daily UVB irradiance is much smaller in September in comparison with June. It was probably due to lower solar elevation angle in autumn, resulting in atmospheric UV absorption (Blumthaler and Ambach 1990). As a consequence, cumulative UVB dose over the course of the egg developmental period is smallest in September. Daily maximum temperature also rapidly decreases in autumn while moderate heat stress is present in early summer (Fig. 5-10a). As a consequence, both of the risks of UVB and high temperature injury are minimized in autumn, leading high egg hatching success. Moreover, monthly precipitation is usually highest in June and July (wet season), possibly reducing egg hatchability and also survival (especially in juveniles) on upper leaf surfaces. *Brevipalpus obovatus* was only recorded on wild VEP plants during the time period corresponding to the autumn peak. These factors may be the main reasons why the *B. obovatus* population only increases in autumn (e.g., Inoue 1960; Sudo et al. 2010).

Chapter 6
General discussion

Phytoseiids, a major acarine predator on forest vegetation (Sudo et al. 2010), constantly stay on lower leaf surfaces or inside domatia, and thus they are rare on upper leaf surfaces (Chapter 2). In contrast, some herbivorous mites such as *P. citri* or *B. obovatus* exploit not only lower but also upper leaf surface (Fukaya et al. 2013; Chapter 2). The utilization of upper leaf surface increases the risk of environmental stress (Ohtsuka and Osakabe 2009; Chapter 5).

Phytoseiid mites are more vulnerable to UVB than herbivorous mites (Tachi and Osakabe 2012). By staying the lower leaf surfaces and inside domatia, phytoseiids can avoid or mitigate the negative effects of environmental stresses such as sunlight or rainfall. Moreover, abundance of their food resources [pollen, fungi and fungivorous mites (e.g., Winterschmidtiidae)] and shelter structures against intraguild predators (domatia and dense hairs) strengthens the priority of lower (abaxial) leaf surface as habitat of phytoseiid mites to upper leaf surface (Jeppson 1975; O'Dowd and Willson 1989; McMurtry and Croft 1997; Kreiter et al. 2003; Chapter 2). Therefore, both of the environmental stress and the bottom-up effects likely drive phytoseiid mites to lower surface-biased distribution on their host leaves.

Consequently, herbivorous mites have probably been facing an evolutional trade-off between the benefit (reduced predator density) and the cost (solar UVB and heat stress) accompanying the upper-surface utilization. Herbivorous mites are expected to develop at least two incompatible life history strategies, which are relevant to their leaf-surface distribution, and possibly to reproductive expenditure.

One is to concentrate most of their resources (e.g., eggs) on the lower leaf surface; many spider mites, especially Tetranychus species, are considered to adopt this strategy. Tetranychus mites usually stay and oviposit on the lower surfaces (Jeppson 1975; Ohtsuka and Osakabe 2009), and their eggs are more vulnerable to UVB than the mites of upper leaf surface user such as *B. obovatus* and *P. citri* (Tachi and Osakabe 2012; Fukaya et al. 2013; Chapter 5). Instead, these lower-surface users belonging to Genus *Tetranychus* exhibit higher reproductive rates (i.e., *r*-strategist) in comparison with the upper-surface users (Saito 1979). Such a higher increasing potential has been considered advantageous to overcome the pressure by specialist predators of Phytoseiidae (Huffaker et al. 1969; Saito 1990) as well as to complete their life cycle on unstable resources e.g., leaves of herbaceous plants (Saito 1979).

In contrast, the life style in *B. obovatus* using both upper and lower surfaces of a single leaf as oviposition sites was evidenced in Chapter 2–5, suggesting another life history strategy than that

described above. An adult female of *B. obovatus* did not lay all of her eggs on the upper side of a VEP leaf, but it oviposits on both upper and lower sides, roughly in accordance with the surface-distribution ratio of the adult individual (Chapter 4).

On leaves, *B. obovatus* balances the environmental stresses (mainly solar UV radiation and radiant heat) with direct and indirect negative effects of phytoseiid mites. Chapter 4 demonstrated *B. obovatus* adults actively changed their leaf-surface distribution to avoid *P. nipponicus*. Behavioral response (avoidance) of *B. obovatus* to UV is not tested directly in this study. However, it is likely that *B. obovatus* adults possess the ability to percept and avoid sunlight including UV, for mites such as phytoseiid mites and spider mites have been known to do so for the orientation on their host leaves (Onzo et al. 2010; Sakai and Osakabe 2010; Tachi and Osakabe 2012; Suzuki et al. 2013). The difference in the upper–lower frequency of *B. obovatus* eggs between on wild VEP leaves (35% on the upper surfaces) and on VEP leaves in laboratory (around 70% on the upper surfaces in both presence/absence of *P. nipponicus*) suggests that *B. obovatus* actually avoid the environmental stresses unique to upper leaf surfaces.

As a conclusion, this study demonstrated that the heterogeneity in physical environment between the upper and the lower surfaces of a VEP leaf segregated the within-leaf distribution of *P. nipponicus* and *B. obovatus*, thereby mitigating their interspecific interaction and making the upper leaf surface an 'enemy-free space' (Jeffries and Lawton 1984) for the prey mite. Nutritional value of the upper (adaxial) leaf surface of VEP was not inferior to the lower (abaxial) leaf surface; fecundity of *B. obovatus* on VEP leaves did not significantly differ between the adaxial and abaxial surfaces if phytoseiid mites were absent (Chapter 3). The predator *P. nipponicus* showed the positive geotaxis and the preference for the surface architecture on the abaxial surface of a VEP leaf (Chapter 4), and the intra-leaf distribution of phytoseiid mites on wild woody plants concentrated on the lower surfaces regardless of seasons and daytime/night (Chapter 2). Thus, oviposition of *B. obovatus* on the leaf upper surface is advantageous in avoiding phytoseiid predators throughout the seasons. On the other hand, the upper-surface utilization increases the risk of environmental stress injury in eggs. *Brevipalpus obovatus* eggs are more protected against UVB and high temperature (radiant heat) than ones of the lower surface users (e.g., *T. urticae*) (Chapter 5). However, both solar UVB and high-temperature stress are considered to reduce *B. obovatus* egg hatchability less than half in the seasons except for autumn (Chapter 5). The seasonal effects in the availability of upper leaf surface would be responsible for the seasonal population dynamics of *B. obovatus*.

The results of the present study, combined with a growing body of evidence on the physiological basis of stress resistance in mites, will deepen our understanding on the function of physical environment (e.g., solar radiation) as a determinant of life-history strategies relevant to the herbivorous mites of Trombidiformes. The maintenance of UVB and/or heat resistance in eggs might impose some fitness cost on the acarine upper-surface users; for instance, the maintenance of UVB resis-

tance in zooplanktons, especially pigmentation with melanin or carotenoids, requires physiological costs (Hessen 1996). Such fitness costs will put a brake on the level of the UVB resistance in mites, as well as the physiological investment in an individual egg to increase the resistance might lead to lower egg production. Furthermore, environmental condition on the upper leaf surfaces might give an incentive to large-size eggs with lower egg production, in terms of preventing desiccation and sunlight penetration through eggshell. As a consequence, an effect of environmental stress on the (possibly *K*-selected) parental investment of the upper-surface users is expected.

References

Adams NK, Shick JM (2001) Mycosporine-like amino acids prevent UVB-induced abnormalities during early development of the green sea urchin *Strongylocentrotus droebachiensis*. *Marine Biol* 138: 267–280.

Adobe Systems Incorporated (2002) Adobe Photoshop Elements. version 2.0. San Jose, California

Barcelo JA (1981) Photoeffects of visible and ultraviolet radiation on the two-spotted spider mite, *Tetranychus urticae*. *Photochem Photobiol* 33: 703–706.

Baskerville GL, Emin P (1969) Rapid estimation of heat accumulation from maximum and minimum temperatures. *Ecology* 50: 514–517.

Bates D, Maechler M, Bolker B (2013) lme4: Linear mixed-effects models using S4 classes. version 0.999999-2. URL http://lme4.r-forge.r-project.org/

Blumthaler M, Ambach W (1990) Indication of increasing solar ultraviolet-B radiation flux in alpine regions. *Science* 248: 206–208.

Broström G, Holmberg H (2011) glmmML: Generalized linear models with clustering. version 0.82-1

Chien JC, Sussex IM (1996) Differential regulation of trichome formation on the adaxial and abaxial leaf surfaces by gibberellins and photoperiod in *Arabidopsis thaliana* (L.) Heynh. *Plant Physiol* 111: 1321–1328.

Duso C, Malagnini V, Paganelli A, Aldegheri L, Bottini M, Otto S (2004) Pollen availability and phytoseiid abundance (Acari: Phytoseiidae) on natural and secondary hedgerows. *BioControl* 49: 397–415.

Ehara S (eds) (1980) *Illustrations of the Mites and Ticks of Japan*. Zenkoku Noson Kyoiku Kyokai, Tokyo (in Japanese).

Ehara S (1962) Notes on some predatory mites (Phytoseiidae and Stigmaeidae). *Jpn J Appl Entomol Zool* 6: 53–60.

Ehara S (eds) (1993) *Plant Mites of Japan in Colors*. Zenkoku Noson Kyoiku Kyokai, Tokyo (in Japanese).

Ehara S, Amano H (2009) *Phytoseius (Dubininellus) nipponicus* Ehara. In Ehara S, Gotoh T (eds.) *Colored Guide to the Plant Mites of Japan*, pp. 96–97. Zenkoku Noson Kyoiku Kyokai, Tokyo (in Japanese).

Ehara S, Gotoh T (2009) *Brevipalpus obovatus*. In Ehara S, Gotoh T (eds.) *Colored Guide to the Plant Mites of Japan*, p. 152. Zenkoku Noson Kyoiku Kyokai, Tokyo (in Japanese).

Foott WH (1963) Competition between two species of mites. II. Factors influencing intensity. *Can Entomol* 95: 45–57.

Fournier V, Rosenheim JA, Brodeur J, Marshall WJ (2004) Population dynamics and within-plant distribution of the mite *Calacarus flagelliseta* (Acari: Eriophyidae) on papaya in Hawaii. *J Econ Entomol* 97: 1563–1569.

Fukaya M, Uesugi R, Ohashi H, Sakai Y, Sudo M, Kasai A, Kishimoto H, Osakabe M (2013) Tolerance to solar ultraviolet-B radiation in the citrus red mite, an upper surface user of host plant leaves. *Photochem Photobiol* 89: 424-431.

Goyal M, Sadana GL, Sharma NK (1985) Influence of temperature on the development of *Brevipalpus obovatus* (Acarina: Tenuipalpidae). *Entomon* 10: 125–129.

Grostal P, O'Dowd DJ (1994) Plants, mites and mutualism: leaf domatia and the abundance and reproduction of mites on *Viburnum tinus* (Caprifoliaceae). *Oecologia* 97: 308-315.

Gutschick VP (1999) Biotic and abiotic consequences of differences in leaf structure. *New Phytol* 143: 3-18.

Hessen DO (1996) Competitive trade-off strategies in arctic *Daphnia* linked to melanism and UV-B stress. *Polar Biol* 16: 573–579.

Huffaker CB, van de Vrie M, McMurtry JA (1969) The ecology of tetranychid mites and their natural control. *Annu Rev Entomol* 15: 125–174.

Ikegami Y, Yano S, Takabayashi J, Takafuji A (2000) Function of quiescence of *Tetranychus kanzawai* (Acari: Tetranychidae), as a defense mechanism against rain. *Appl Entomol Zool* 35: 339–343.

Inoue K (1960) Seasonal prevalence and control measures of two spider mite species on *Rhododendron* No. 2 (original title: ツツジに寄生する2種のハダニの発生消長とその防除 第2報). *Proc Assoc Pl Prot Kyushu* 6: 48–49 (in Japanese).

Izaguirre MM, Mazza CA, Svatoš A, Baldwin IT, Ballaré CL (2007) Solar ultraviolet-B radiation and insect herbivory trigger partially overlapping phenolic responses in *Nicotiana attenuata* and *Nicotiana longiflora*. *Ann Bot* 99, 103-109.

Jeffries MJ, Lawton JH (1984) Enemy free space and the structure of ecological communities. *Biol J Linn Soc* 23: 269–286.

Jeppson LR (1975) Chapter 2. Population ecology. In: Jeppson LR, Keifer HH, Baker EW (eds) *Mites Injurious to Economic Plants*, pp. 17–46. University of California Press, Berkeley, California.

Johnson HB (1975) Plant pubescence: an ecological perspective. *Bot Rev* 41: 233–258.

Jones VP, Parrella MP (1984) Intratree regression sampling plans for the citrus red mite (Acari: Tetranychidae) on lemons in southern California. *J Econ Entomol* 77: 810–813.

Kalthoff K (1975) Compensation for solar UV damage by solar radiation of longer wavelengths (Smittia spec., Chironomidae, Diptera). *Oecologia* 18: 101–536.

Karban R, English-Loeb G, Walker MA, Thaler J (1995) Abundance of phytoseiid mites on *Vitis* species: effects of leaf hairs, domatia, prey abundance and plant phylogeny. *Exp Appl Acarol* 19: 189–197.

Kasai A, Yano S, Takafuji A (2005) Prey–predator mutualism in a tritrophic system on a camphor tree. *Ecol Res* 20: 163–166.

Kiritani K (2012) The low development threshold temperature and the thermal constant in insects and mites in Japan (2nd edition). *Bull Natl Inst Agro-Environ Sci* 31: 1–74 (in Japanese).

Kiritani K (2013) Different effects of climate change on the population dynamics of insects. *Appl Entomol Zool* 48: 97–104.

Kreiter S, Tixier MS, Croft BA, Auger P, Barret D (2002) Plants and leaf characteristics influencing the predaceous mite *Kampimodromus aberrans* (Acari: Phytoseiidae) in habitats surrounding vineyards. *Environ Entomol* 31: 648–660.

Kreiter S, Tixier M-S, Bourgeois T (2003) Do generalist phytoseiid mites (Gamasida: Phytoseiidae) have interactions with their host plants? *Insect Sci Appl* 23: 35–50.

Krips OE, Kleijn PW, Willems PEL, Gols GJZ, Dicke M (1999) Leaf hairs influence searching efficiency and predation rate of the predatory mite *Phytoseiulus persimilis* (Acari: Phytoseiidae). *Exp Appl Acarol* 23: 119–131.

Li J, Margolies DC (1991) Factors affecting location of Banks grass mite, *Oligonychus pratensis* (Acari: Tetranychidae), on corn leaves. *Exp Appl Acarol* 12: 27–34.

Loughner R, Goldman K, Loeb G, Nyrop J (2008) Influence of leaf trichomes on predatory mite (*Typhlodromus pyri*) abundance in grape varieties. *Exp Appl Acarol* 45: 111–122.

Loughner R, Wentworth K, Loeb G, Nyrop J (2010) Leaf trichomes influence predatory mite densities through dispersal behavior. *Entomol Exp Appl* 134: 78–88.

Macfadyen EJ, Williamson CE, Grad G, Lowery M, Jeffrey WH, Mitchell DL (2004) Molecular response to climate change: temperature dependence of UV-induced DNA damage and repair in the freshwater crustacean *Daphnia pulicaria*. *Glob Change Biol* 10: 408–416.

McFadden D (1974) Conditional logit analysis of qualitative choice behavior. In: Zarembka P (ed.) *Frontiers in Econometrics*, pp. 105–142. Academic Press, New York.

McMurtry JA, Croft BA (1997) Life styles of phytoseiid mites and their roles as biological control agents. *Annu Rev Entomol* 42: 291–321.

Murata Y, Osakabe M (2013) The Bunsen-Roscoe reciprocity law in ultraviolet-B-induced mortality of the two-spotted spider mite *Tetranychus urticae*. *J Insect Physiol* 59: 241–247.

Newsham KK, Low MNR, McLeod AR, Greenslade PD, Emmett BA (1997) Ultraviolet-B radiation influences the abundance and distribution of phylloplane fungi on pedunculate oak (*Quercus robur*). *New Phytol* 136: 287–297.

Nishida S (2004) Morphology and function of domatia. *Bunrui* 4: 137-150 (in Japanese).

Norton AP, English-Loeb G, Belden E (2001) Host plant manipulation of natural enemies: leaf domatia protect beneficial mites from insect predators. *Oecologia* 126: 535–542.

O'Dowd DJ, Pemberton RW (1998) Leaf domatia and foliar mite abundance in broadleaf deciduous forest of north Asia. *Am J Bot* 85: 70–78.

O'Dowd DJ, Willson MF (1989) Leaf domatia and mites on Australasian plants: ecological and evolutionary implications. *Biol J Linn Soc* 37: 191–236.

O'Dowd DJ, Willson MF (1997) Leaf domatia and the distribution and abundance of foliar mites in broadleaf deciduous forest in Wisconsin. *Am Midl Nat* 137: 337–348.

Ohtsuka K, Osakabe Mh (2009) Deleterious effects of UV-B radiation on herbivorous spider mites: they can avoid it by remaining on lower leaf surfaces. *Environ Entomol* 38: 920–929.

Okabe K (2006) Astigmatid mites damaging agricultural crops (1). *Plant Protection* 60: 233–236 (in Japanese).

Onzo A, Hanna R, Zannou I, Sabelis MW, Yaninek JS (2003) Dynamics of refuge use: diurnal, vertical migration by predatory and herbivorous mites within cassava plants. *Oikos* 101: 59–69.

Onzo A, Hanna R, Sabelis MW (2009) Within-plant migration of the predatory mite *Typhlodromalus aripo* from the apex to the leaves of cassava: response to day–night cycle, prey location and prey density. *J Insect Behav* 22: 186–195.

Onzo A, Sabelis MW, Hanna R (2010) Effects of ultraviolet radiation on predatory mites and the role of refuges in plant structures. *Env Entomol* 39: 695–701.

Osakabe M (1967) Biological studies on the tea red spider mite, *Tetranychus kanzawai* Kishida, in tea plantation. *Bull Tea Res Sta* 4: 35–156 (in Japanese).

Price CE (1980) A review of the factors influencing the penetration of pesticides through plant leaves. In: Cutler DF, Alvin KL, Price CE (eds) *Plant cuticle, papers presented at an International Symposium organized by the Linnean Society of London, held at Burlington House, London, 8-11 September 1980*, pp. 237–252. Academic Press, London.

R Development Core Team (2009) R: A language and environment for statistical computing, version 2.10.1. R Foundation for Statistical Computing, Vienna.

R Core Team (2012) R: A language and environment for statistical computing, version 2.15.1. R Foundation for Statistical Computing, Vienna.

Ripley B, Venables B, Hornik K, Gebhardt A, Firth D (2012) MASS: support functions and datasets for Venables and Ripley's MASS. version 7.3-22. http://cran.r-project.org/web/packages/MASS/index.html

Roda A, Nyrop J, Dicke M, English-Loeb G (2000) Trichomes and spider-mite webbing protect predatory mite eggs from intraguild predation. *Oecologia* 125: 428–435.

Roda A, Nyrop J, English-Loeb G, Dicke M (2001) Leaf pubescence and two-spotted spider mite webbing influence phytoseiid behavior and population density. *Oecologia* 129: 551–560.

Roda A, Nyrop J, English-Loeb G (2003) Leaf pubescence mediates the abundance of non-prey food and the density of the predatory mite *Typhlodromus pyri*. *Exp Appl Acarol* 29: 193–211.

Roy M, Brodeur J, Cloutier C (2003) Effect of temperature on intrinsic rates of natural increase (r_m) of a coccinellid and its spider mite prey. *BioControl* 48: 57–72.

Saito Y (1979) Comparative studies on life histories of three species of spider mites (Acarina: Tetranychidae). *Appl Entomol Zool* 14: 83–94.

Saito Y (1985) Life types of spider mites. In: Helle W, Sabelis MW (eds.) *Spider Mites. Their Biology, Natural Enemies and Control, Vol. 1A*, pp. 253–264. Elsevier, Amsterdam.

Saito Y (1986) Prey kills predator: counter-attack success of a spider mite against its specific phytoseiid predator. *Exp Appl Acarol* 2: 47–62.

Saito Y (1990) Life-history and feeding habit of *Typhlodromus bambusae*, a specific predator of *Schizotetranychus celarius* (Acari: Phytoseiidae: Tetranychidae). *Exp Appl Acarol* 10: 45–51.

Sakai Y, Osakabe Mh (2010) Spectrum-specific damage and solar ultraviolet radiation avoidance in the two-spotted spider mite. *Photochem Photobiol* 86: 925–932.

Sakai Y, Sudo M, Osakabe M (2012a) A comparison of the effects of gravity and the nutritional advantage of leaf surfaces on fecundity in the two-spotted spider mite (Acari: Tetranychidae). *J Acarol Soc Jpn* 21: 1–6.

Sakai Y, Sudo M, Osakabe M (2012b) Seasonal changes in the deleterious effects of solar ultraviolet-B radiation on eggs of the twospotted spider mite, *Tetranychus urticae* (Acari: Tetranychidae). *Appl Entomol Zool* 47: 67–73.

Santos CD (2005) Photoreactivation of ultraviolet-B damage in *Tyrophagus putrescentiae* (Acari: Acaridae) and *Tetranychus urticae* (Acari: Tetranychidae). *Internat J Acarol* 31: 429–431.

Sinha RP, Häder D-P (2002) UV-induced DNA damage and repair: a review. *Photochem Photobiol Sci* 1: 225–236.

Stavrinides MC, Mills NJ (2011) Influence of temperature on the reproductive and demographic parameters of two spider mite pests of vineyards and their natural predator. *BioControl* 56: 315–325.

Stenseth C (1979) Effect of temperature and humidity on the development of *Phytoseiulus persimilis* and its ability to regulate populations of *Tetranychus urticae* [Acarina: Phytoseiidae. Tetranychidae]. *Entomophaga* 24: 311–317.

Sudo M, Nishida S, Itioka T (2010) Seasonal fluctuations in foliar mite populations on *Viburnum erosum* Thunb. var. *punctatum* Franch. et Sav. (Adoxaceae) and sympatric shrubs in temperate secondary forests in western Japan. *Appl Entomol Zool* 45: 405–415.

Suzuki T, Watanabe M, Takeda M (2009) UV tolerance in the two-spotted spider mite, *Tetranychus urticae*. *J Insect Physiol* 55: 649–654.

Suzuki T, Kojima T, Takeda M, Sakuma M (2013) Photo-orientation regulates seasonal habitat selection in the two-spotted spider mite, *Tetranychus urticae*. *J Exp Biol* 216: 977–983.

Tachi F, Osakabe M (2012) Vulnerability and behavioral response to ultraviolet radiation in the components of a foliar mite prey-predator system. *Naturwissenschaften* 99: 1031–1038.

Tanaka M, Inoue K (1962) The study for forecasting *Panonychus citri*. No. 4. The nature of rainfall that affects the population density of spider mites. Analysis by simulated rain. *Proc Assoc Pl Prot Kyushu* 8: 18–20 (in Japanese).

Ullah MS, Haque MA, Nachman G, Gotoh T (2012) Temperature-dependent development and reproductive traits of *Tetranychus macfarlanei* (Acari: Tetranychidae). *Exp Appl Acarol* 56: 327–344.

van Haren RJF, Steenhuis MM, Sabelis MW, Ponti OMB de (1987) Tomato stem trichomes and dispersal success of *Phytoseiulus persimilis* relative to its prey *Tetranychus urticae*. *Exp Appl Acarol* 3: 115–121.

Venables WN, Ripley BD (2002) *Modern Applied Statistics with S. 4th edn.* Springer, New York.

Villanueva RT, Childers CC (2005) Diurnal and spatial patterns of Phytoseiidae in the citrus tree canopy. *Exp Appl Acarol* 35: 269–280.

Walter DE (1996) Living on leaves: mites, tomenta, and leaf domatia. *Annu Rev Entomol* 41: 101–114.

Walter DE, Behan-Pelletier V (1999) Mites in forest canopies: filling the size distribution shortfall? *Annu Rev Entomol* 44: 1–19.

Walter DE, Proctor HC (1999) *Mites: ecology, evolution, and behaviour.* CABI Publishing, Wallingford, Oxon.

Watanabe H (1997) Estimation of arboreal and terrestrial arthropod densities in the forest canopy as measured by insecticide smoking. In: Stork NE, Adis J, Didham RK (eds) *Canopy Arthropods*, pp. 401–414. Chapman & Hall, London.

Weintraub PG, Kleitman S, Alchanatis V, Palevsky E (2007) Factors affecting the distribution of a predatory mite on greenhouse sweet pepper. *Exp Appl Acarol* 42: 23–35.

Acknowledgements

First of all, I would like to express sincere gratitude to my honorable supervisors in Graduate School of Agriculture, Kyoto University: Dr. Hiroshi Amano, Dr. Masahiro Osakabe and Dr. Shuichi Yano, for their excellent guidance as well as tolerance and respect for academic freedom. I would like to express my special gratitude to Dr. Osakabe for his unusual patience. Moreover, I would not hit upon the basic idea of this work —the utilization of upper leaf surfaces as a means of predator avoidance— without his epoch-making finding on the solar-UVB effects on mites.

My special gratitude also goes to my former teachers in my master's course in Graduate school of Human and Environmental Studies, Kyoto University: Dr. Takao Itioka and Dr. Makoto Kato, for their kind help and suggestions in the germination term of the present study. I was encouraged by their deep insights and enthusiasm to ecology and natural history. I also thank Dr. Sachiko Nishida, who gave me the first break of my field research on mites on forest trees.

I would like to take this opportunity to thank acarologists and entomologists for their voluntary supports: Dr. Kimiko Okabe for the identification of winterschmidtiid mites, Dr. Yutaka Saito and Dr. Keizi Kiritani for valuable comments to Chapters 3 and 5 in this work, respectively, and editors and anonymous reviewers of my published works.

Thanks are also extended to academic/clerical staffs and students of Division of Environmental Science and Technology, Graduate school of Agriculture, and Department of Interdisciplinary Environment, Graduated school of Human and Environmental Studies, both at Kyoto University, for their expertise and supports to my study. I owe Ms. Tomoko Nakanishi a debt of gratitude for taking trouble especially in ordering consumables. I also would like to thank Dr. Keiko Kishimoto-Yamada, Dr. Satoshi Yamashita and Dr. Atsushi Kasai for their constructive criticisms of the early phase of my study life. Mr. Yuta Sakai gave me valuable suggestions on the experimental procedures using UV.

I am grateful to fellows of Kyoto University Wildlife Research Association, and Yakushima Macaque Research Group, not only for their expertise and suggestions but also longstanding friendship.

I express my gratitude to Japan Society for the Promotion of Science (JSPS) research fellowship (Grant-in-Aid for JSPS Fellows Nos. 23.2696) for supporting this study.

Thanks are also extended to the R Foundation for Statistical Computing, and developers of add-on libraries used in the statistical analyses of this study. The solar UV radiation dataset used in this study was provided by Solar Radiation and Weather Monitoring Project, Kyoto Woman's University. The long-term temperature data was provided by the Kyoto Local Meteorological Observatory, Japan Meteorological Agency. This work could be accomplished without such free

software and open data. I also thank participants in Panasonic Corporation for providing and setting UVB lamp used in the experiment in Chapter 5.

Last, but not least, I would like to express my sincerest thanks to my father Yoshio Sudo, my mother Toshiko Sudo and my brother Hirotaka Sudo, for their irreplaceable support and resolute faith in my career-path selection.